# Dynamic Earth Energy Storage: Terawatt-Year, Grid-Scale Energy Storage using Planet Earth as a Thermal Battery (GeoTES): Seedling Project Final Report

Travis L. McLing, Dan Wendt, Patrick Dobson, Christine Doughty, Nic Spycher, Dakota Roberson, and J. Fred McLaughlin

May 2019

**INL**
**Idaho National Laboratory**

# Dynamic Earth Energy Storage: Terawatt-Year, Grid-Scale Energy Storage using Planet Earth as a Thermal Battery (GeoTES): Seedling Project Final Report

Travis L. McLing, Dan Wendt, Patrick Dobson, Christine Doughty, Nic Spycher, Dakota Roberson, and J. Fred McLaughlin

May 2019

Idaho National Laboratory
Idaho Falls, Idaho 83415

http://www.inl.gov

# SUMMARY

Grid-scale energy storage has been identified as a needed technology to support the continued build-out of intermittent renewable energy resources. As of April 2017, the U.S. had approximately 24.2 GW of energy storage on line, compared to 1,081 GW of installed generation capacity (Litynski et al. 2006, Hellström 2003). This represents a large shortfall of the storage needed to stabilize the U.S. grids with the rising penetration of renewable energy. Our team proposed to address this shortfall through the storage of excess energy as geothermal brine in deep geologic formations. This concept, known as geologic thermal energy storage (GeoTES), relies on the storage of thermal energy in geologic formations for recovery and use in large-scale direct use geothermal applications. As such, GeoTES has the potential to play a significant role in meeting the energy storage shortfall in the coming decades by assisting with peak demand ramping, easing stress on transmission, providing regional storage to support sustainable direct use geothermal applications, and providing a variety of grid stabilization benefits due to renewable outages or inaccurate forecasting and rotor stability.

# CONTENTS

# FIGURES

# TABLES

# ACRONYMS

GeoTES         geologic thermal energy storage

FWH            feed water heater

HP              high pressure

IP               intermediate pressure

LP              low pressure

MCL          minimum compliant load

MSD          mass spring damper

RTES         Regional Thermal Energy Storage

SMIB.        Single Machine Infinite Bus

TES           thermal energy storage

WI              Western Interconnect

WECC        Western Electric ordinating Council

# Dynamic Earth Energy Storage: Terawatt-Year, Grid-Scale Energy Storage using Planet Earth as a Thermal Battery (GeoTES): Seedling Project Final Report

## 1. INTRODUCTION

Grid-scale energy storage has been identified as a needed technology to support the continued build-out of intermittent renewable energy resources. As of April 2017, the U.S. had approximately 24.2 GW of energy storage on line, compared to 1,081 GW of installed generation capacity (Litynski et al. 2006). This represents a large shortfall of the storage needed to stabilize the U.S. grids with the rising penetration of renewable energy. The project team (Idaho National Laboratory, Lawrence Berkeley National Laboratory, University of Idaho, and University of Wyoming) proposed to address this shortfall through the storage of excess energy as geothermal brine in deep geologic formations. This concept, known as geologic thermal energy storage (GeoTES), relies on the storage of thermal energy in geologic formations for recovery and use in large-scale direct use geothermal applications. As such, GeoTES has the potential to play a significant role in meeting the energy storage shortfall in the coming decades by assisting with peak demand ramping, easing stress on transmission, providing regional storage to support sustainable direct use geothermal applications, and providing a variety of grid stabilization benefits due to renewable outages or inaccurate forecasting and rotor stability.

This GeoTES approach addressed the preliminary science, engineering, and technical issues associated with large-scale day to seasonal storage and recovery of excess energy for large scale deep direct use geothermal applications (Figure 1). This evaluation included siting criteria and model performance of potential geologic energy storage reservoirs, how power plants would respond to charging and later utilizing these thermal energy storage (TES) systems, and then seeing how such a system would impact grid stability. The four areas the project team focused the initial study include:



Figure 1. Schematic depiction of GeoTES within an integrated energy network.

- Geologic setting for GeoTES reservoirs

- Subsurface thermo-hydrological and chemical modeling of reservoir performance and sustainability

- Evaluation of increase in steam Rankine cycle ramping capacity due to storage of excess steam

- GeoTES grid stability – modeling implications.

Because suitable geologic formations are located across the U.S., large-scale GeoTES is a vehicle that allows for national buildout of geothermal energy, through capture and direct use of excess thermal energy Rankine power stations during periods when production exceeds load requirements. Given the size, extent, and distribution of deep saline aquifers in North America, the amount of energy that can be stored is enormous and enough to provide the grid balancing needed for increased renewable energy penetration.

This seedling study has the following components: (1) initially evaluate representative deep sedimentary basins that have been previously characterized for carbon capture and storage (e.g., Illinois, Williston Basin, etc.); (2) evaluate the increase in steam Rankine cycle ramping capacity due to storage of excess steam; (3) conduct preliminary modeling work to assess the energy efficiency of TES and retrieval

1

for both direct use (thermal) and electrical power generation; and (4) characterize the potential impact on grid-wide rotor stability.

## 2. GEOLOGIC SETTING FOR GEOTES

As detailed in Section 1, this study focused on developing and testing the feasibility of coupling fluctuations of the energy supply between renewable and nonrenewable power sources to develop deep geothermal energy storage sites in a low temperature reservoir(s). Ideally, the site would offer multiple geologic reservoir types to model injection and storage responses relative to dynamic geology. This geologic assessment for thermal storage focused on conventional formations that are typical in most sedimentary basins that are distributed across much of the U.S., specifically carbonate and sandstone reservoirs. With respect to carbonates, the project team narrowed the search for those reservoirs that had been dolomitized (limestone converted to dolomite). These are more likely to have uniform porosity and permeability over limestone, as they are a byproduct of formation-wide crystallization instead of the random dissolution. In turn, this simplifies the reservoir modeling with respect to fluid flow dynamics. The project team anticipated that using a highly heterogenous vuggy limestone model would not provide defendable results. With respect to sandstone reservoirs, the search focused to either eolian systems and/or thick offshore marine sands that can accumulate along passive margins. The project team favored these sands, over fluvial sands, as they typically have better storage capacities as well as being more mature (i.e., higher percentage of quartz to clay, which is better suited for fluid injection). This feasibility study has identified sandstone maturity (i.e., the amount of quartz volume relative to reactive grains) as being one of the more important variables for maintaining the effectiveness of long-term thermal storage (see Section 3 and 4).

For this initial evaluation of candidate formations in and near Wyoming, the oldest is the Mississippian Madison Limestone, which was extensively dolomitized prior to deep burial, particularly across the western half of Wyoming. Carbonate reservoirs of similar age and character are identified across the western U.S., the Great Plains from Canada through Texas, as well as portions of sedimentary basins in the south and southeastern U.S. Other formations examined (the Weber and Nugget sandstones) include both sandstones but vary significantly with respect to reservoir quality and vary slightly with respect to mineralogy. The Weber Sandstone is comprised mostly of quartz, with calcite, dolomite, and anhydrite cements and minor feldspar, pyrite, and heavy accessory minerals (McLaughlin and Garcia-Gonzalez 2013). In western Wyoming, the Weber Sandstone has a basal lithology that is dominantly marine, and is generally tight and unusable for fluid injection, and an upper lithology that is dominantly eolian with better reservoir qualities (i.e., porosity and permeability) (McLaughlin and Garcia-Gonzalez 2013). The Weber has lesser reservoir qualities (i.e., lower porosity and permeability) of all three targeted reservoirs due to quartz dissolution and subsequent cementation, which is a common feature in thick sands found worldwide. The Nugget Sandstone is a relatively clean quartz sandstone, though it is not as mature as the Weber Sandstone. Unlike the Weber, the Nugget has relatively minor amounts of cement, resulting in better reservoir properties and increased effectiveness of fluid injection. Both Weber and the Nugget are relatively mature sandstones. Such sandstones have been identified as an important variable for successful, long-term fluid injection, as these formations are more resilient to mineral alteration and ensuing formation damage.

In addition to identifying common reservoir types that would be analogous in many basins worldwide, the field of study was narrowed to include proximity to a power station (thermal source) as well as areas that had available data and weren't actively producing hydrocarbons from these formations (recognizing that oil and gas producers in Wyoming have primacy regarding reservoir usage). This led us to select an area near the Jim Bridger Power Station for study, which is on the northeastern flank of the Rock Springs Uplift (Figure 2). Jim Bridger Power Station is the largest coal plant in Wyoming and is adjacent to one of the largest wind farms under development in North America (Figure 3). Previous subsurface studies at Jim Bridger Power Station have evaluated the region's potential for commercial carbon capture utilization and storage CCUS. These studies produced large datasets, including seismic

data, petrophysical data, reservoir fluid data and core, which greatly increases the ability to develop realistic property models (Jiao et al. 2017). Specifically, these previous studies collected and evaluated a seismic cube that encompasses a 16 mi$^2$ area, a suite of geophysical logs from a deep science well and surrounding plugged and abandoned wells, a suite of core analysis from over 900' ft of core that detailed reservoir character, temperature, pressure, and geochemical data from two of these formations, and existing geologic property models that can be adapted to test (Figure 4). These studies detailed the impact of large-scale fluid injection within the Madison and Weber reservoirs (Hunter et al. 2017; Jiao et al. 2017) and show that millions of tons of fluids could safely be injected into the reservoir without formation damage or risk to sealing formations.
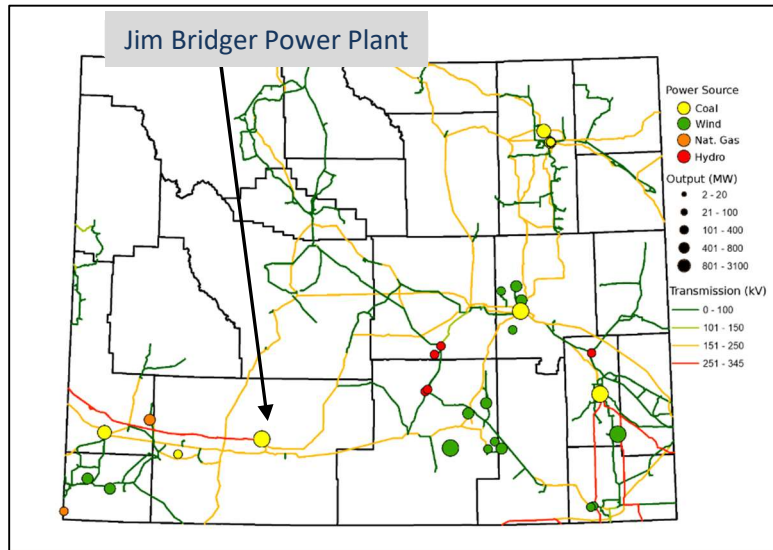
Figure 2. Energy infrastructure in Wyoming, including coal, wind, natural gas, and hydro power generators with associated output and transmission infrastructure.

Figure 3. Archean provinces in Wyoming: note that the majority of the state is underlain by Archean rocks including major sedimentary basins http://waterplan.state.wy.us/basins/7basins.html).
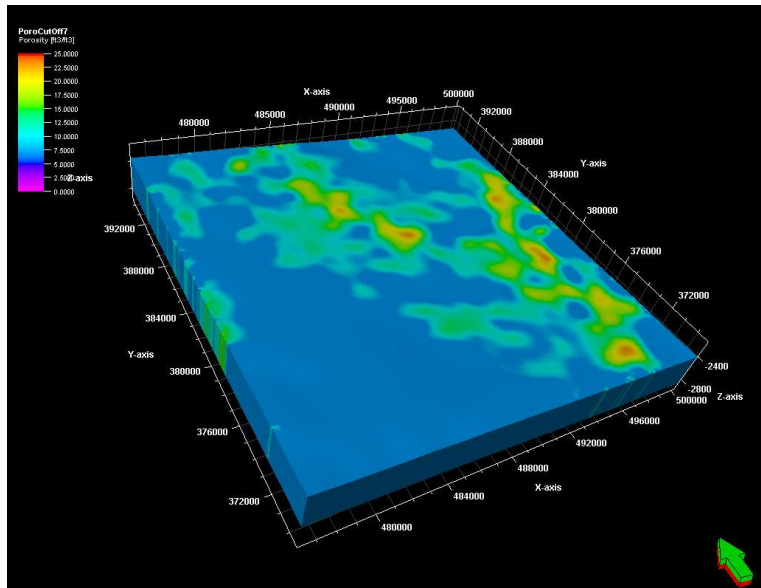


Figure 4. Detailed porosity map of a horizon in the Nugget Sandstone generated using available data collected from the Rock Springs Uplift (Surdam et al. 2011).

# 3. SUBSURFACE THERMO-HYDROLOGICAL MODELING OF GEOTES

After selecting a potential host formation for GeoTES, the next component of this seedling project was to evaluate the potential performance reservoir thermal energy storage. To illustrate the subsurface fluid flow and thermal behavior during GeoTES, a series of simple models are developed based on an annual storage cycle. Each cycle includes hot water injection for three summer months when there is a surplus of hot water, a three-month rest period in fall when energy supply and demand are balanced, water production for three months in winter when hot water demand is high, and another three-month rest period in spring. This cycle is repeated for 10 years.

The proposed storage reservoir, the Weber/Tensleep Formation in the Rock Springs Uplift, is approximately 200 m thick and occurs at depths of 3400–3600 m. Hydrologic layering was simplified from Rock Springs Uplift well log interpretations of density porosity, and is illustrated in Figure 13, which shows a vertical cross-section through the model. Thermal conductivity, 1.3 W/mK, is taken from literature values. Initial conditions are a brine-saturated formation with a salinity of 50,000 ppm, and hydrostatic pressure and geothermal temperature gradients that yield P ~ 3.5 MPa and T~94$^\circ$C at formation depth. The salinity value was selected based on a range of values presented by Stauffer et al. 2009 on $CO_2$ sequestration in the Rock Springs Uplift, where they quoted salinity as 35,000–80,000 ppm. This differs from the higher salinity value (~100,000 ppm) obtained from F. McLaughlin for the geochemical modeling work – this difference will have a negligible effect on the thermal hydraulic simulations.

The injection/production rate is chosen to be the maximum rate for which pressure remains below the frac pressure during injection and above the boiling point during production. The initial injection temperature is specified at ~160°C. The injection enthalpy is held fixed, so as pressure increases during injection, the temperature declines correspondingly.

## 3.1 Thermal-Hydrological Model

The coupled fluid flow and heat flow in the storage reservoir are numerically simulated using TOUGH3, with the equation of state EOS7, which considers a water-brine-heat system. Although TOUGH3/EOS7 can handle two-phase (liquid water, steam) flow, the present problem is single-phase liquid. Heat loss to the cap and bedrock are modeled with a semi-analytical solution, so no grid is needed beyond the storage reservoir.

Three well geometries are considered: (1) a single-well push-pull system, in which the same well is used for injection and production; (2) an isolated injection-well/production-well pair; and (3) an injection-well/production-well pair within a field of many such pairs in a five-spot pattern (Figure 13). The first two geometries include a laterally extensive model to represent an infinite system, whereas the third geometry has closed (no-flow) lateral boundaries, to represent the symmetry of the five-spot pattern. All three grids have the same vertical discretization and layering.

The grid shown in Figure 5 is for the single-well RZ model. Radial grid spacing is finer over the expected extent of the thermal plume. The actual grid extends much farther radially than shown, with ever-coarsening grid spacing, to represent an infinite aquifer for the pressure simulation. The total number of grid blocks in the radial direction is 38 and there are 20 layers, for a total of 760 grid blocks. This small number of grid blocks arises from the assumption of radial symmetry, which allows a two-dimensional (RZ) grid to model three-dimensional space.

The isolated injection-well/production-well pair model is an XYZ grid that represents one well pair in a grid that extends far laterally in all directions. Because there are two separate wells, radial symmetry no longer applies, but only half of the domain need be modeled, with the line between the two wells acting as an axis of symmetry. As for the RZ grid, the region close to the wells is discretized more finely than more

distant regions. The total number of grid blocks per layer is 6,250 and there are 20 layers, for a total of 125,000 grid blocks, which is substantial. The grid refinement is designed so well separations of 14, 28, and 39 m can be considered.

The five-spot grid represents one injection-well/production-well pair in a field of many such pairs. By symmetry, only $1/8^{th}$ of the problem needs to be discretized (Figure 6) and it requires far fewer grid blocks because it is closed on all sides, which represent symmetry boundaries. The five-spot grid is also locally refined around the wells and has only 73 grid blocks per layer and there are 20 layers, for a total of 1,460 elements. Well separation is 28 m.
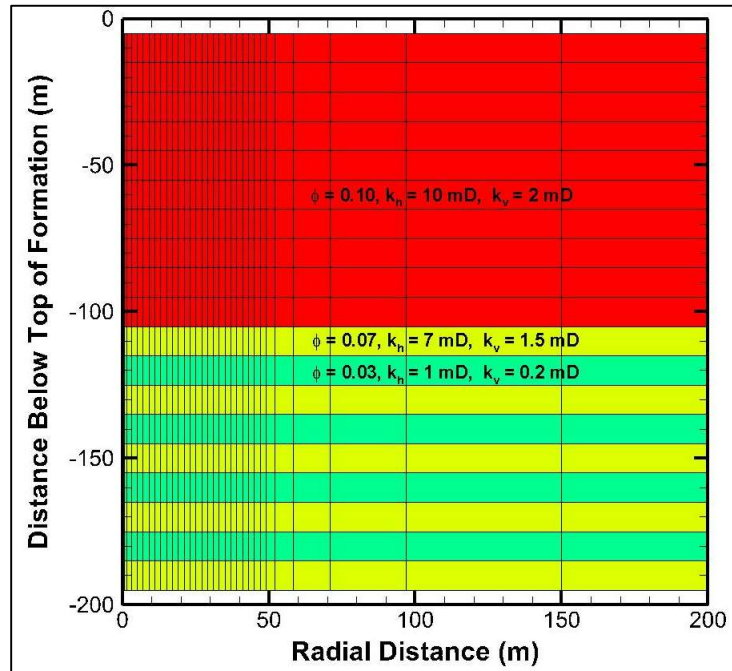


Figure 5. Vertical cross-section through the RZ model, showing the vertical discretization, and material property assignments for all three models.
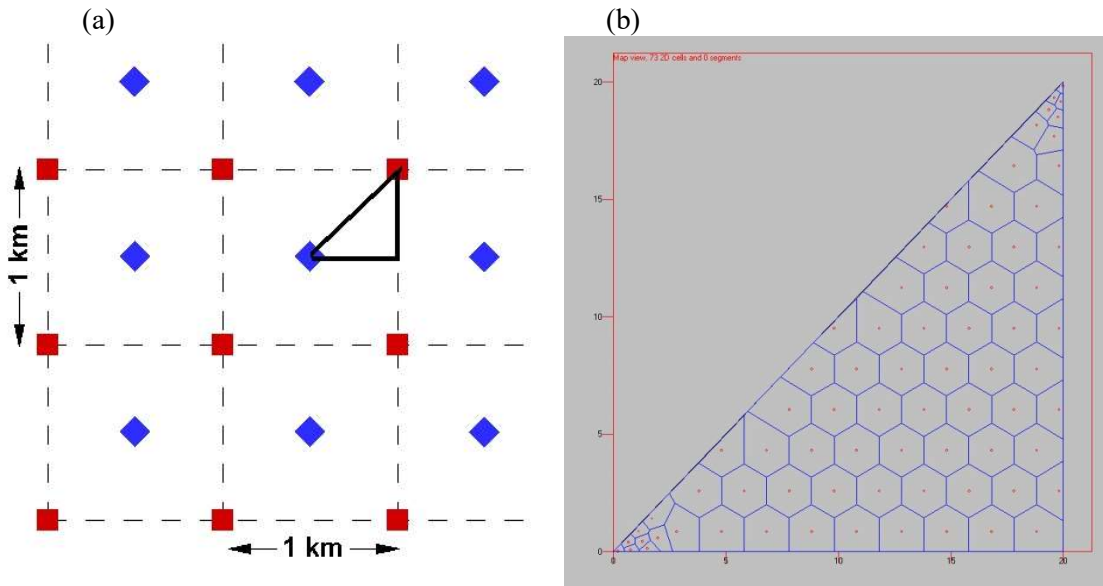
Figure 6. (a) Schematic view of the five-spot problem, in which many injection-well (blue)/ production-well (red) pairs exist. The dashed lines delineate individual five-spot patterns. The solid black line shows the 1/8th symmetry element required to model the system. (b) Plan view of the five-spot grid. The injection well is at (0,0) and the production well is at (20,20).

For the isolated injection-well/production-well pair model, which is laterally extensive, only one well pumps at a time: the injection well during summer and the production well during winter, in a straightforward adaption of the single-well push-pull schedule. This pumping schedule does not work for the closed five-spot model, as pressure increases too much in summer and decreases too much in winter. To maintain pressure within desired limits, the two wells must always have very nearly equal and opposite pumping rates. During summer, the production well provides the water that is heated by the power plant then injected; its pumping draws the hot injected water toward it. During winter, the injection well takes the produced water after most of its heat is extracted for end use and injects it, pushing moderate temperature water toward the production well, behind the stored hot water injected the previous summer. Besides modulating pressure changes, this schedule eliminates the need for supplemental water to be provided for injection or produced water to be disposed of after its heat has been extracted.

The key result of the 10-year simulations is a plot of production temperature as a function of time, with injection temperature also shown for reference (Figure 7). The injection (inlet) temperature (first quarter of each year) varies between 150 and 160°C for all cases, with smaller variation for smaller pressure change. Small spikes in injection and production temperature often are visible when pumping starts or stops; these are due to the Joule-Thomson effect, which produces a small temperature increase when pressure drops and a small temperature decrease when pressure increases.
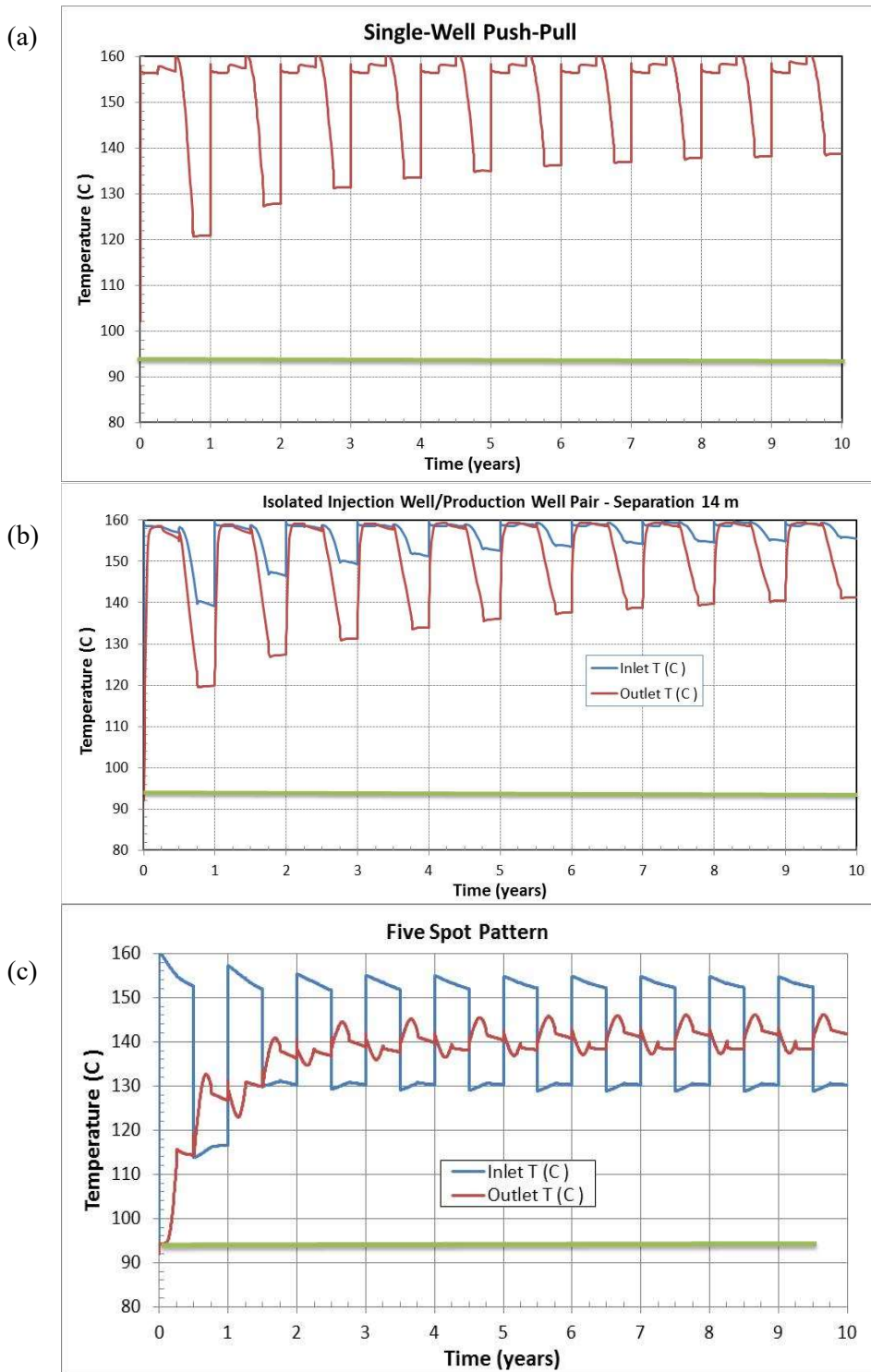
Figure 7. Inlet temperature and outlet temperature for (a) RZ model, (b) isolated injection-well/production-well pair with a well separation of 14 m, (c) five-spot pattern. The green line shows the average initial reservoir temperature.

For the single-well push-pull and isolated well pair with 14-m well separation, production (outlet) temperature drops from 160°C to 120°C during the first-year production period. There is a gradual improvement for the first five years, then a steady state develops with production temperature dropping

8

from 160°C to 140°C each cycle. This large production temperature range is a problem for incorporating GeoTES into power-plant operations, which requires nearly constant temperature water.

For the five-spot pattern, pumping rates for each well pair must be lower than for the single well and isolated well pairs, since the closed lateral boundaries preclude the pressure dissipation seen in the laterally extensive models. But because many well pairs are presumed to exist, each one having a lower pumping rate makes sense. The resulting smaller flow rates are expected to be advantageous for geochemistry. After the first three years, production temperature stays in the range of 141°C to 146°C. During each third-quarter production period, the production temperature gradually increases, then declines, with the peak occurring when the thermal front passes the production well. After some trial and error, it was found that making the well separation somewhat bigger than the extent of the thermal plume yields a production temperature with the smallest range of variation, which is important for power-plant operations.

For the isolated well pair with a well separation of 14 m, the well separation is smaller than the extent of the thermal plume, so the production temperature starts out equal to the injection temperature (red and blue lines in Figure 7b nearly overlap at the start of the production period). Two additional simulations of isolated well pairs were done, with well separations of 28 and 39 m. The production temperatures are shown in Figure 4. For these larger well separations, the production temperature starts out lower than the injection temperature, although the difference decreases for later cycles. But the range of production temperature is at least as big as for the smaller well separation (Figure 7b), so there does not appear to be any advantage to using a larger well separation.

In conclusion, these different models for seasonal RTES would all be viable if only subsurface thermo-hydrologic behavior were of interest. But because geochemical effects are a primary concern for long-term RTES, the symmetry features that enable the RZ and five-spot models to have far fewer grid blocks makes them much more practical for the computationally intensive simulations including geochemistry. Furthermore, if we consider how the subsurface behavior interacts with the power plant, the need for a nearly constant outlet temperature makes the five-spot pattern most appealing.
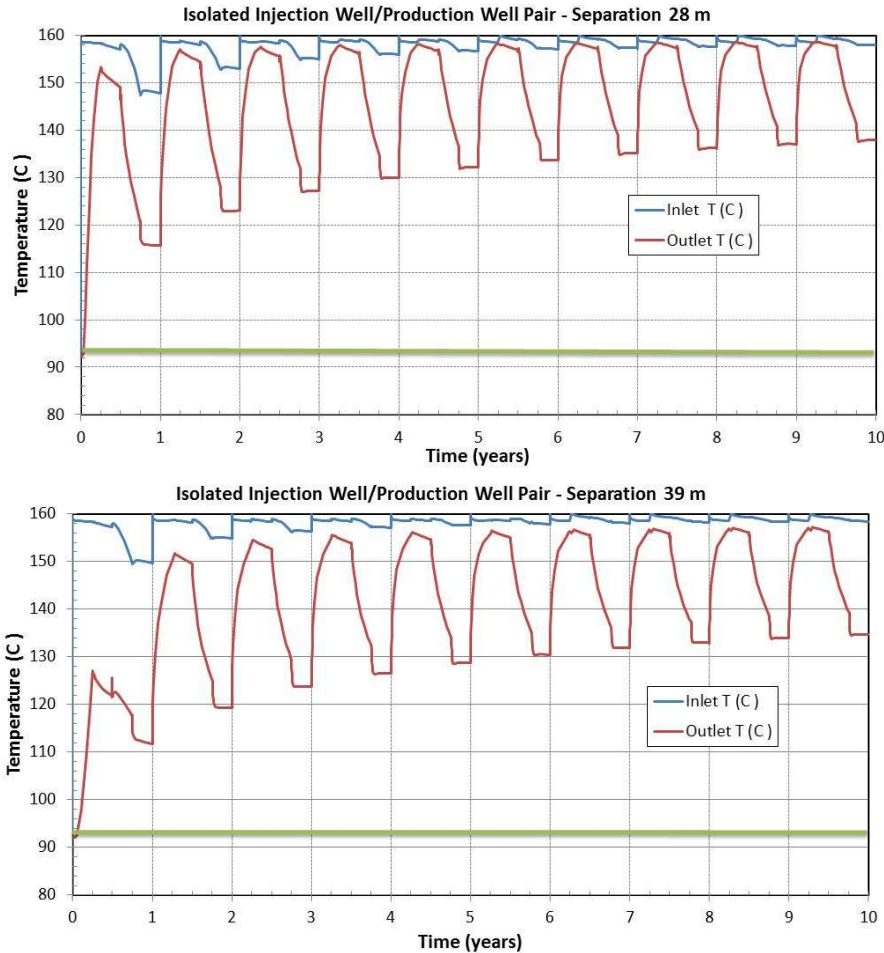
Figure 8. Inlet temperature and outlet temperature for isolated injection-well/production-well pairs with a well separation of (a) 28 m and (b) 39 m. The green line shows the average initial reservoir temperature.

## 4. GEOCHEMICAL AND REACTIVE TRANSPORT MODEL

Based on the thermal-hydrological model presented in Sections 2 and 3, geochemical and reactive transport simulations were carried out to investigate the chemical aspects of the TES system, including mineral precipitation and dissolution as these may potentially affect TES operations. These simulations were performed with a newly developed (and U.S. Department of Energy Geothermal Technology Office-funded) version of Lawrence Berkley National Laboratory's in-house reactive transport simulator (TOUGHREACT-Brine), which has the capability of computing ion activities in highly saline solutions. This modeling work was based on water chemical analyses from the Weber Formation (Sample C12120562-001 12/14/12 21:00, courtesy F. McLaughlin), with a total dissolved solid concentration around 100,000 mg/L (Table 1).

The provided water analysis was compared with other data for the Weber Formation from the U.S. Geological Survey Produced Water Database, for samples with similar total dissolved solid concentration, to ensure that these data fell in line with other reported analyses for this formation. The formation water composition at depth was then reconstructed by geochemical modeling to account for $CO_2$ loss and cooling effects, yielding a slightly more acidic pH (~5.5) and higher total carbonate content (~4500 mg/L) than shown in Table 1. The deep-water composition was also reconciled with mineralogical data for the Weber Formation obtained from the literature, yielding close equilibrium with phases either known to be present in this formation, or reasonably expected to occur. These minerals include calcite, dolomite, siderite, anhydrite, illite, chalcedony, and Fe sulfides.

In a first step, the effect of heating the formation water from its in-situ temperature near 94 to 160°C (the injection temperature considered in the thermal-hydrological model) was modeled using the grid depicted in Figure 5. The goal of this exercise was to evaluate the amount of salt precipitation resulting from simply heating the extracted brine (before its re-injection). Figure 9 shows that anhydrite and carbonate minerals would be expected to precipitate (on the order of several kg/m³ brine).

Table 1. Analysis of water from the Weber Formation used in geochemical and reactive transport simulations.

| Species | Units | Measured Concentration |
|---|---|---|
| pH | | 6.46 at 25C |
| density (kg/L, calc) | | 1.079 |
| | | |
| Cl- | mg/L | 57400 |
| SO4-2 | mg/L | 6030 |
| HCO3- | mg/L | 3996 |
| HS- | mg/L | 127 |
| Si | mg/L | 45 |
| Al+3 | mg/L | 3.5 |
| Ca+2 | mg/L | 539 |
| Mg+2 | mg/L | 45 |
| Fe+2 | mg/L | 44 |
| K+ | mg/L | 1910 |
| Na+ | mg/L | 36500 |
| Sr+2 | mg/L | 14 |
| F- | mg/L | 6.1 |
| B | mg/L | 72 |
| Br- | mg/L | 99 |
| Ba+2 | mg/L | 14 |
| Li+ | mg/L | 91 |
| NH3 (as N) | mg/L | 33 |
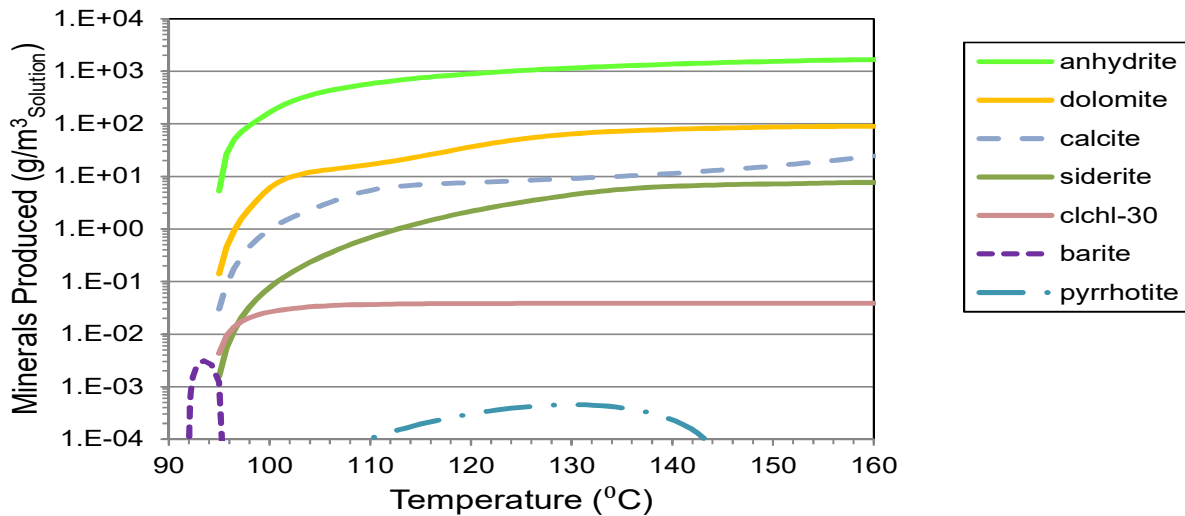


Figure 9. Computed amounts of minerals precipitated by (ex-situ) heating of the extracted formation water.

Reactive transport simulations of injection were then performed using the heated brine (160°C) depleted of the minerals precipitated upon heating. These simulations were run using the same thermal-hydrological model described earlier for the case of the single-well push-pull system, including identical numerical mesh and input thermal-hydrological parameters. Results show (Figure 10) significant precipitation of calcite close to the injection well, which largely dominates small amounts of anhydrite dissolution and thus results in a significant near-well permeability decrease. The precipitation of calcite is explained by the retrograde solubility of this mineral (i.e., solubility decrease with increasing temperature), which then results in (in-situ) calcite precipitation when the formation water around the injection well heats up from the re-injection of hot water. The minor dissolution of anhydrite around the injection well is attributed to the fact that this mineral was depleted from the extracted water (by heating, Figure 5) before its reinjection.
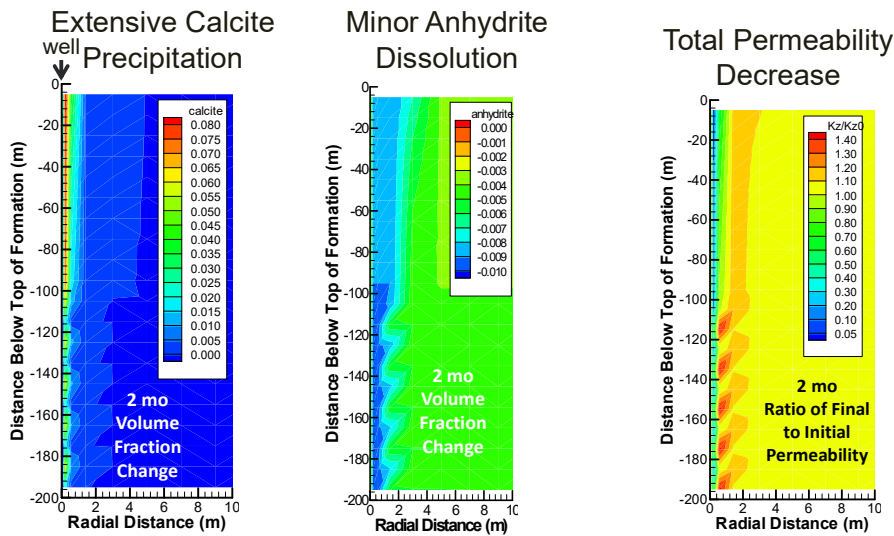


Figure 10. Mineral precipitation (calcite) and dissolution (anhydrite) with effect on permeability (overall decrease) computed for a two-month simulated injection period.


## 5.   POWER SYSTEM MODELING: EVALUATION OF INCREASE IN STEAM RANKINE CYCLE RAMPING CAPACITY UPON INTEGRATION WITH A GEOTES SYSTEM

Increased deployment of intermittent renewable energy sources introduces potential mismatches between electrical supply and demand, which can result in destabilization of the electrical grid. The goal of this portion of our study is to investigate GeoTES technology as a medium for storing thermal energy when electricity demand is low, and to recover the stored energy to provide enhanced energy resources using existing thermo-electric power plants when demand is high. The power plant analysis task of this project had the objectives to (1) identify approaches for diverting thermal energy away from steam Rankine cycle power plants and into TES during periods of low energy demand and for adding thermal energy recovered from storage into the power plant during periods of high energy demand, and (2) quantify the impact of the heat removal and heat addition operations on power plant net power generation for the purpose of providing enhanced power ramping capacity.

Diverting heat away from conventional thermo-electric power plants during periods of low energy demand would allow the plants to remain online with reduced electrical power output while continuing to

provide rotational inertia for stabilization of the electrical grid. The diverted heat would be used to charge the GeoTES system, and the stored heat could be recovered and utilized to boost power plant output during periods of high energy demand.

In Phase I of this Beyond Batteries project, GeoTES and steam Rankine cycle power plant thermal integration was investigated. Specifically, a coal-fired power plant configuration was examined. Coal-fired power plants utilize mature and widely deployed technology with several large plants present in the geographic area of interest for the Phase I analysis in the Western U.S. (Figure 1). Coal-fired plant shutdowns are occurring primarily for economic reasons (fuel costs, regulatory/infrastructure upgrades, etc.); however, these closures will result in reduction in the power plant technologies that provide large rotational inertia that inherently stabilizes the electrical grid. Information regarding the configuration and operation of coal-fired power plants is readily available, and coal-fired power plants provide numerous heat integration options. Although the Phase I power plant analysis focused on coal-fired power plants, the findings and results of this analysis are also applicable to other steam Rankine cycle power plants (nuclear, fuel oil, gas combined cycle plant, coal-to-gas conversions, integrated gasification combined cycle, etc.).
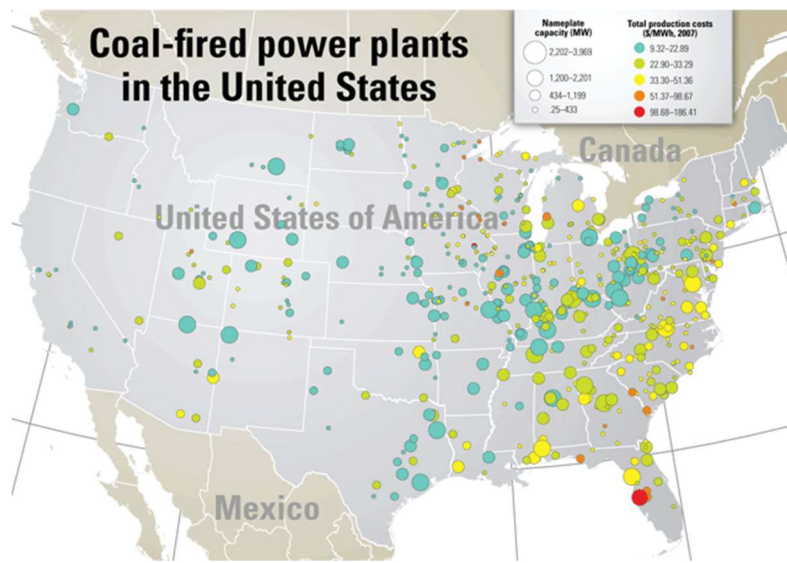


Figure 11. Coal-fired power plants in the U.S. (Image Source: Power Magazine).

## 5.1 Steam Rankine Cycle Heat Export

Several options exist for exporting heat from steam Rankine cycles. This analysis limited investigation to existing piping and/or heat transfer systems within steam Rankine cycle plants, i.e., introduction of all new heat transfer systems into existing power plants was not considered practical or necessary and therefore was not explored.

Potential options include use of existing power plant systems including (a) the steam extraction system (in current plants this system is used to provide steam to the boiler feed water heat exchangers), (b) the steam bypass system (used primarily for plant startup and shutdown purposes), or (c) the flue gas heat recuperation system. Additional discussion for each option is provided in subsequent sections.

## 5.2 Heat Recovery via the Steam Extraction System

An initial investigation of heat export via the steam extraction system (i.e., the boiler feed water heating system) concluded that the quantity of heat that could be exported from the plant did not provide

sufficient heat input into the GeoTES system nor was it adequate to significantly reduce the power output from the plant.

## 5.3　Flue Gas Heat Recovery

Although heat from the flue gas could be exported to a GeoTES system, it would be impractical to recover this high-temperature heat for use in the lower temperature GeoTES system for thermodynamic reasons (underutilization of the high grade heat source) as well as practical reasons (the heat exchangers would have to withstand the high temperature environment on the flue gas side, which would require more expensive materials of construction, and the use of high temperature heat would increase the chances of mineral fouling on the brine side of the heat exchanger). Further, extracting heat from the flue gas system would not support exporting quantities of heat sufficient to significantly decrease electrical power output, and because the flue gas heat is normally recovered to provide final preheating of the boiler feed water, much of the reduction in power plant output would come at the cost of decreased plant efficiency.

## 5.4　Heat Recovery via the Steam Bypass System

The steam bypass system appears to provide an excellent pathway for exporting heat from steam Rankine cycle power plants. As previously mentioned, steam bypass systems exist in current steam Rankine cycle plants for startup and shutdown purposes. During startup, the steam extraction system is used to bypass the turbines as the boiler and power cycle piping are heated to operational temperatures before supporting the gradual increase in the flow rate of steam to the turbines. During shutdown, the steam bypass system is used to divert steam away from the turbines if the power plant 'trips' in response to an event that results in operation that is outside of authorized ranges (e.g., regulatory, safety, or equipment performance limitations).

Two types of steam bypass systems are in use: parallel and cascade bypass systems. Both types of bypass systems include the controls, valves, piping, and water quench (using condensate) equipment required to divert steam around the steam turbines and into the condensate recovery system. The cascade bypass system (Figure ) is more prevalent as it does not require a steam Rankine cycle reheater to operate in a "dry" state, which requires use of more expensive high temperature construction materials. Either the parallel or cascade bypass system would be amenable to diverting heat to a GeoTES system.
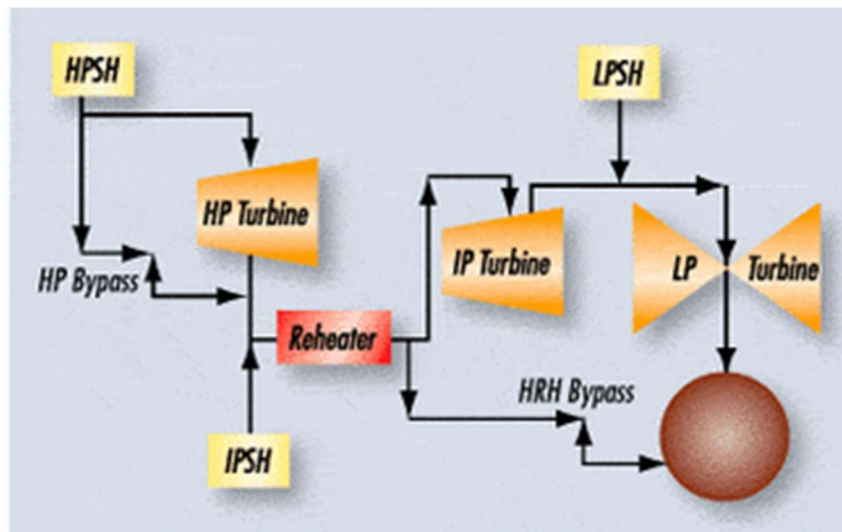


Figure 12. Cascade steam bypass system (Source: Power Engineering www.power-eng.com).

Additional heat exchange equipment could be added to the steam bypass system in order to divert heat to GeoTES brine. A GeoTES system is expected to operate at a much lower temperature than that of

the steam Rankine cycle boiler; prior to heat exchange with the GeoTES brine the steam temperature would be reduced to minimize heat exchanger surface fouling (from minerals in the brine). The steam temperature would be modulated through use of a reheat attemperators, which spray steam-cycle condensate into the bypass flow to simultaneously reduce the temperature and increase the mass flow rate of the steam prior to heat exchange with the brine.

Since the heat output to a GeoTES system would occur at a temperature lower than the low pressure (LP) turbine inlet temperature, in concept it would be possible to first send the high pressure (HP) steam through the HP steam turbine before diverting a portion of the flow to the intermediate pressure (IP) and LP turbine bypass piping. This would provide the most economical use of the steam Rankine cycle fuel (coal, nuclear, etc.) during periods that heat was diverted to the GeoTES system.

However, the HP, IP, and LP turbines are often installed on the same shaft. The torque induced on the shaft by operating the HP and IP/LP turbines at different output levels could result in operational issues including mechanical fatigue as well as potential oscillations in the frequency of the alternating current electrical power output from the plant. Therefore, in Phase I of the project, it was assumed that the steam bypass system is operated in a mode that results in equal steam flow reductions to the HP and IP/LP turbines. Detailed operational analysis and evaluation of full load HP turbine operation with simultaneous partial load IP/LP turbine operation are planned for Phase II of the project.

## 5.5   Steam Rankine Cycle Heat Import

The energy stored in a GeoTES system could be used to enhance power plant performance during times when the net electrical load is high. In order to increase power generation during periods of peak load, a method for importing the heat recovered from the GeoTES system must be established.

Steam Rankine cycles typically have several boiler feed water heaters (FWHs) that heat the condensate before it is vaporized in the boiler. Boiler feed water heating provides internal heat transfer within the power cycle that improves power plant efficiency. Boiler feed water heating allows the high grade heat generated in the boiler to be used primarily for high temperature heat transfer such that lower grade heat (in the form of steam extracted from the turbines) can be used to provide the lower temperature heat transfer to the feed water (steam condensate).

Steam Rankine cycle typically have several boiler FWHs configured in series (Figure ). The first FWH uses low pressure steam to provide low temperature heat input to the condensate, while the last FWH typically uses intermediate or high pressure steam to heat the pressurized feed water to an elevated temperature (several hundred degrees below saturation; high temperature heat from the boiler exhaust gas may also be used as a heat source for feedwater heating).
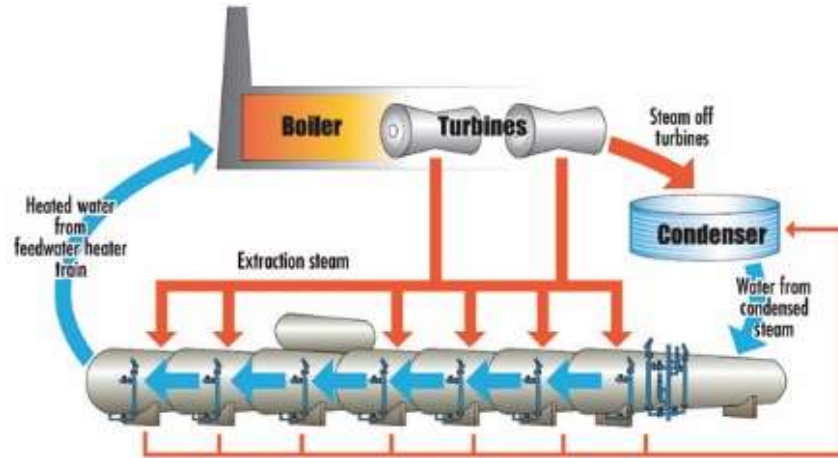
Figure 13. Boiler feed water heating using turbine steam extractions (Source: https://www.magnetrol.com/sites/default/files/styles/paragraph_image/public/blog/feedwater_heater_train .png?itok=mCfrGyh2).

Unfortunately, the steam extracted from the turbines for feed water heating cannot also be used for power generation. However, it would be possible to modify the boiler feed water heating system to provide heat input using the hot brine recovered from the GeoTES system as the heat source instead of steam extracted from the power cycle. Reducing the quantity of steam extracted from the power cycle would allow this steam to instead be used for power generation (by increasing the flow rate of steam expanded through the turbines), which would enhance the ability of the power plant to ramp up power generation during periods of high electrical demand.

The boiler FWHs are positioned in series, each having a higher steam inlet temperature than the preceding unit. As a result, the feed water is heated to a higher temperature as it passes through each sequential FWH. The number of FWHs that could be converted to use brine recovered from a GeoTES system instead of steam therefore depends on the temperature of the recovered brine; higher temperature brine could offset the steam usage in a greater number of FWHs, with a corresponding increase in the electrical power generation. Provided a sufficient flow rate of brine is available, the amount of additional power generation that could be achieved from using GeoTES brine as the source of FWH heat will increase with the temperature at which the GeoTES brine is supplied.

This analysis evaluates the effect of GeoTES brine temperature on steam Rankine cycle power plant net power generation. For each temperature selected, the [increase in] power plant output as a function of brine flow rate is determined (there are practical considerations associated with transporting large volumes of brine). The analysis assumes that turbines and generator ratings will accommodate the additional power generation that would occur upon reducing turbine steam extractions for boiler feed water heating.

## 5.6   Methods

Models of a generic 715 MW$_e$ nameplate capacity subcritical coal power plant unit were developed using IPSEpro v7.0 process modeling software. The capacity of the coal-fired power plant unit modeled is consistent with the size of power generation units in coal-fired power plants in the geographic region of interest (Table 2). Separate models were developed to investigate the off-design power plant performance in both the GeoTES heat export operating mode (using the steam bypass system, Figure ) as well as in the GeoTES heat import operating mode (using the boiler feed water system, Figure ). These models were used to evaluate the impact of heat addition and removal on power generation for selected brine temperatures as well as flow rates.

Table 2. Capacity of selected coal-fired power plants in the geographic region of interest (Western U.S.).

| Plant Name | Total Capacity (MW$_e$) | Units |
|---|---|---|
| Generic coal plant model | 715 | 1 |
| Jim Bridger | 2,318 | 4 |
| Colstrip | 2,272 | 4 |
| Dave Johnston | 817 | 4 |
| Laramie River Station | 1,710 | 3 |
| WyoDak | 402 | 1 |
| Comanche Generating Station | 1410 | 3 |
| Naughton | 707 | 3 |
| Cherokee Station | 801 | 4 |
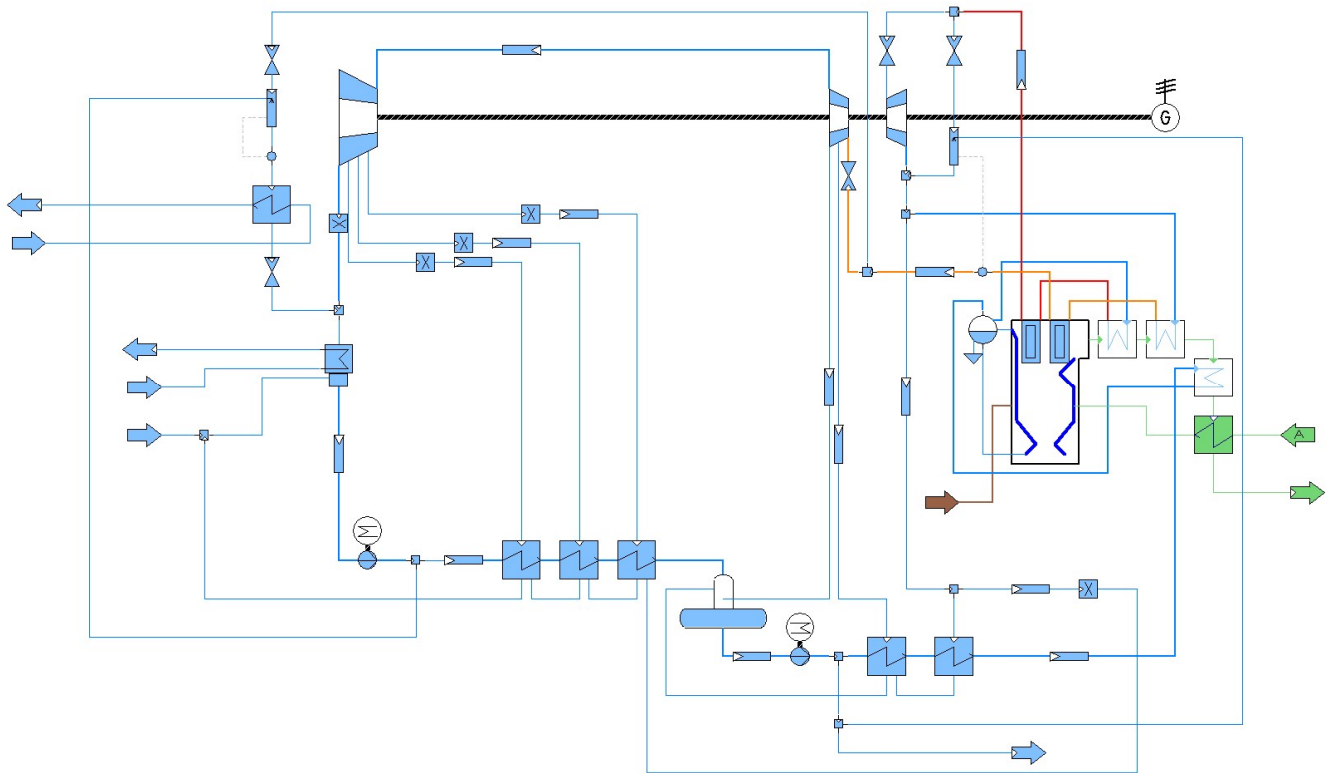


Figure 14. Process flow diagram of coal-fired power plant with GeoTES heat export via steam bypass system (cascade bypass).
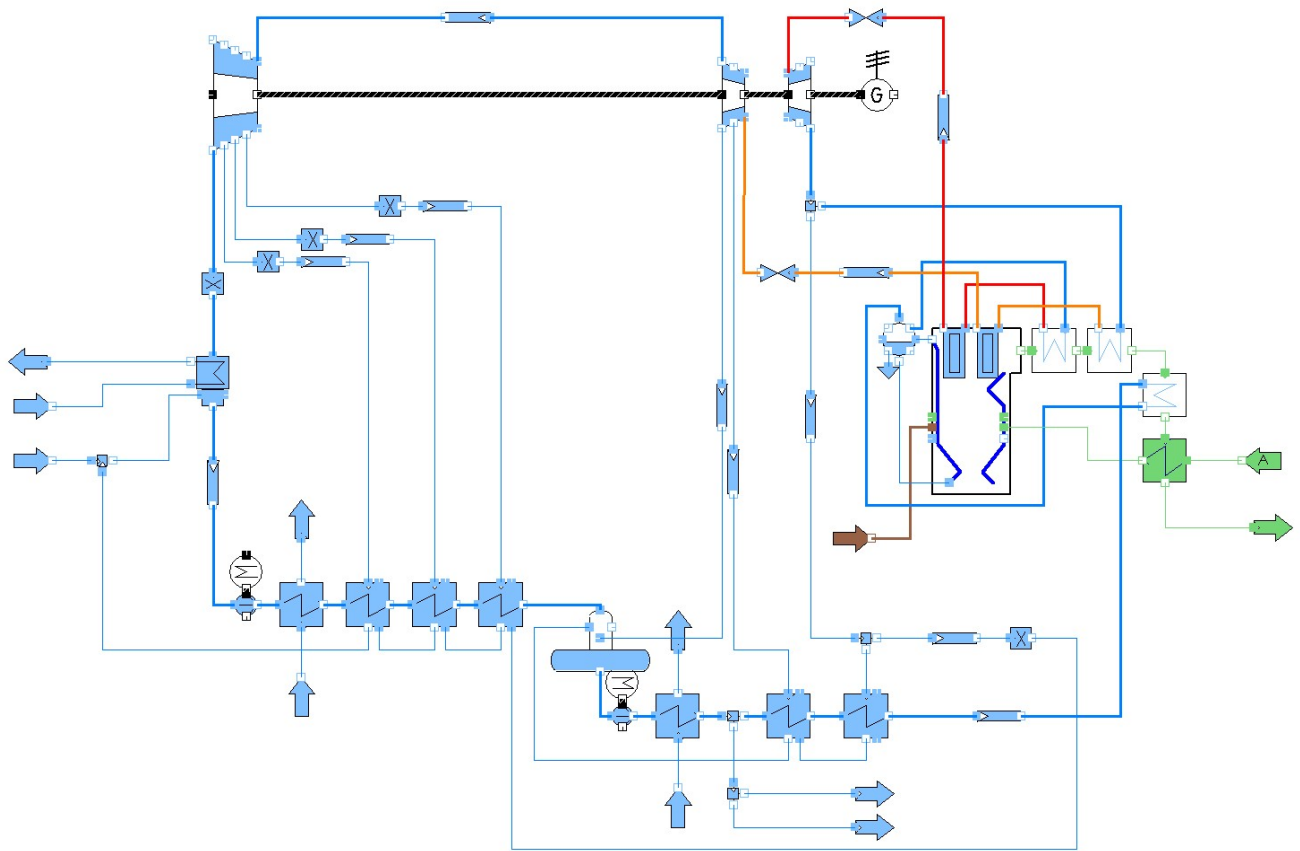
Figure 15. Process flow diagram of coal-fired power plant with GeoTES FWH heat input.

When using the model to determine the minimum power output possible while keeping the power plant operational, it was assumed that the power plant must operate at or above its minimum compliant load (MCL). MCL is the minimum load at which the power plant is complaint either with emissions or other restrictions (Gonzalez-Salazar et al. 2018). This analysis assumes that the power plant must operate at an MCL of 50% boiler output to remain in compliance with operational and regulatory constraints.

The heat export model (Figure ) varied the fraction of the total steam flow rate entering the steam bypass system to evaluate the effect on net power generation. GeoTES brine outlet temperatures ranging from 140°C to 260°C were specified and the model was used to determine the brine flow rates required to condense the steam bypass flow. The plant net power output as a function of GeoTES brine flow rate was evaluated at a boiler load of 50% (corresponding to the assumed MCL).

The heat import model (Figure ) calculated the flow rate of hot GeoTES brine required to eliminate the turbine steam extractions for providing boiler feed water heat input. GeoTES heat recovery temperatures of 120°C to 240°C were evaluated. As the specified temperature of the GeoTES brine was increased, the heating duty for a greater number of FWHs is provided by GeoTES brine instead of extracted steam. Table  describes the FWHs that obtained heat input from GeoTES brine instead of extracted steam as a function of GeoTES brine temperature.

Table 3. FWHs with heating duty provided from GeoTES recovered brine.

| GeoTES brine recovery temperature | FWHs with heating duty provided by recovered GeoTES brine |
|---|---|
| 120°C | FWHs #1 and 2 |
| 160°C | FWHs #1, 2, and 3 |
| 200°C | FWHs #1, 2, 3, and deaerator |
| 240°C | FWHs #1, 2, 3, deaerator, 4, and 5 |

## 5.7    Results and Discussion

The heat export model was used to calculate the coal-fired plant net power output as a function of exported GeoTES brine flow rate and temperature (Figure 11). Since heat would be exported to the GeoTES system during periods when the electrical demand was low, the boiler load was set to its assumed MCL of 50% in order to reduce electrical power output. As can be observed from Figure 11, using the steam bypass system to reduce the electrical power generation and export thermal energy to the GeoTES brine allows the net power output of the plant to be reduced significantly.

Figure 11 illustrates that when the steam bypass system is used to heat the exported brine to a higher temperature, a decreased flow rate of brine is required to achieve a specified reduction in net power generation. Since the capital costs and pumping power requirements for transporting brine increase with flow rate, it would be advantageous to export brine at the highest temperatures possible. However, the geochemistry and thermal performance of the GeoTES system are dependent on operating temperature, and the heat export specifications must therefore be chosen based on acceptable GeoTES operating conditions.

While operating in this low output (heat export) mode, the plant remains operational and coupled to the electrical grid such that the rotational inertia of the steam turbines may continue to provide a stabilizing force for damping frequency variations in the grid. Exporting brine to the GeoTES system could reduce the power plant minimum net power generation from 315 MWe (without heat export) to 125 MWe (with heat export).
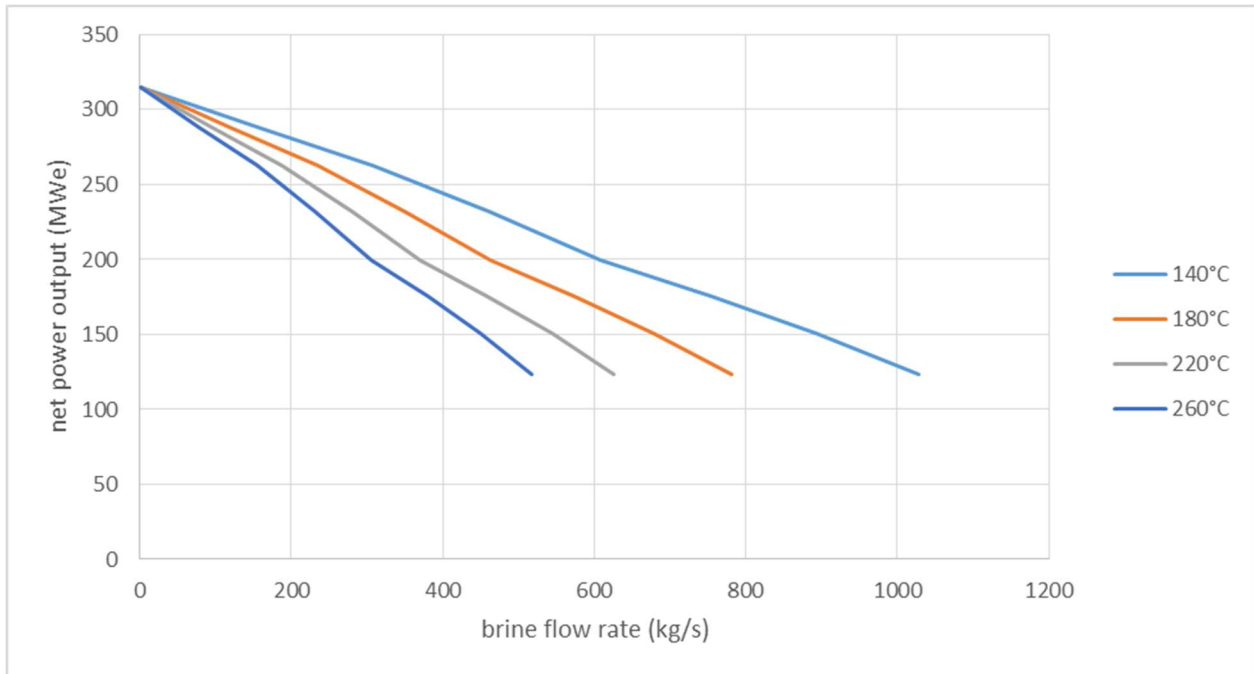
Figure 11. Simulated net power generation of 715 MW$_e$ nameplate capacity coal-fired plant as a function of exported GeoTES brine flow rate and temperature (results presented for MCL of 50% boiler load corresponding to operation during periods of low electrical power demand).
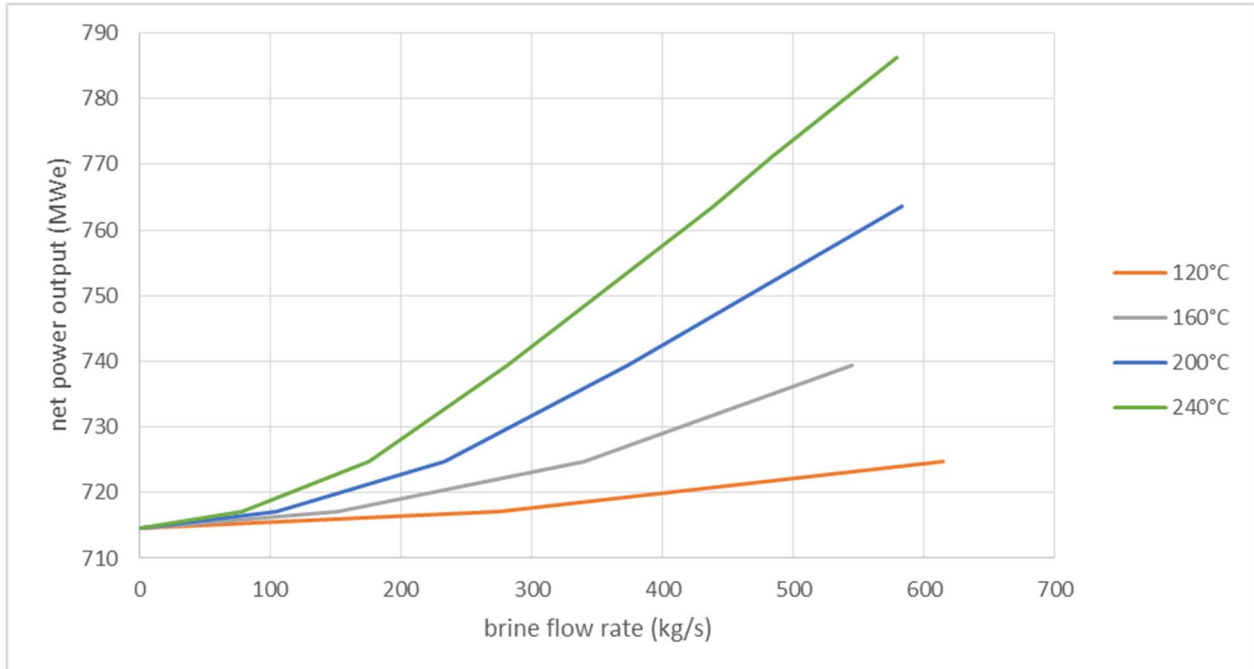


Figure 12. Simulated net power generation of 715 MW$_e$ nameplate capacity coal-fired plant as a function of imported GeoTES brine flow rate and temperature (results presented at 100% boiler load corresponding to operation during periods of high electricity demand).

The heat import model was used to calculate the coal-fired plant net power output as a function of imported GeoTES brine flow rate and temperature (Figure 12). Heat would be imported to the power plant from the GeoTES system during periods of high electrical power demand; during these periods maximal power generation is required, and 100% boiler load is required. As illustrated in Figure 12, use of imported GeoTES heat to supply boiler feed water heating duty could increase the net power generation from the plant during time periods of high electrical power demand.

As the temperature of the GeoTES brine increases, more FWHs can utilize the GeoTES heat, more steam can be expanded through the turbines instead of extracted for feed water heating, and more net power can be produced. For a specified GeoTES brine recovery temperature, increased brine flow rate will provide the heating duty to replace the steam heat input to a greater number of FWHs. However, though GeoTES brine at 240°C is hot enough to provide heat input to FWH #5 (the highest temperature FWH), if only a small flow rate of 240°C brine is available (e.g., 75 kg/s in Figure 12) it would not be able to replace all heat input from steam extractions in FWHs 1 through 5. Therefore, to maximize the benefit of the recovered GeoTES brine, the brine flow rate must be sufficient to provide the heating duty required to replace the steam extractions in all FWHs with applicable operating temperatures.
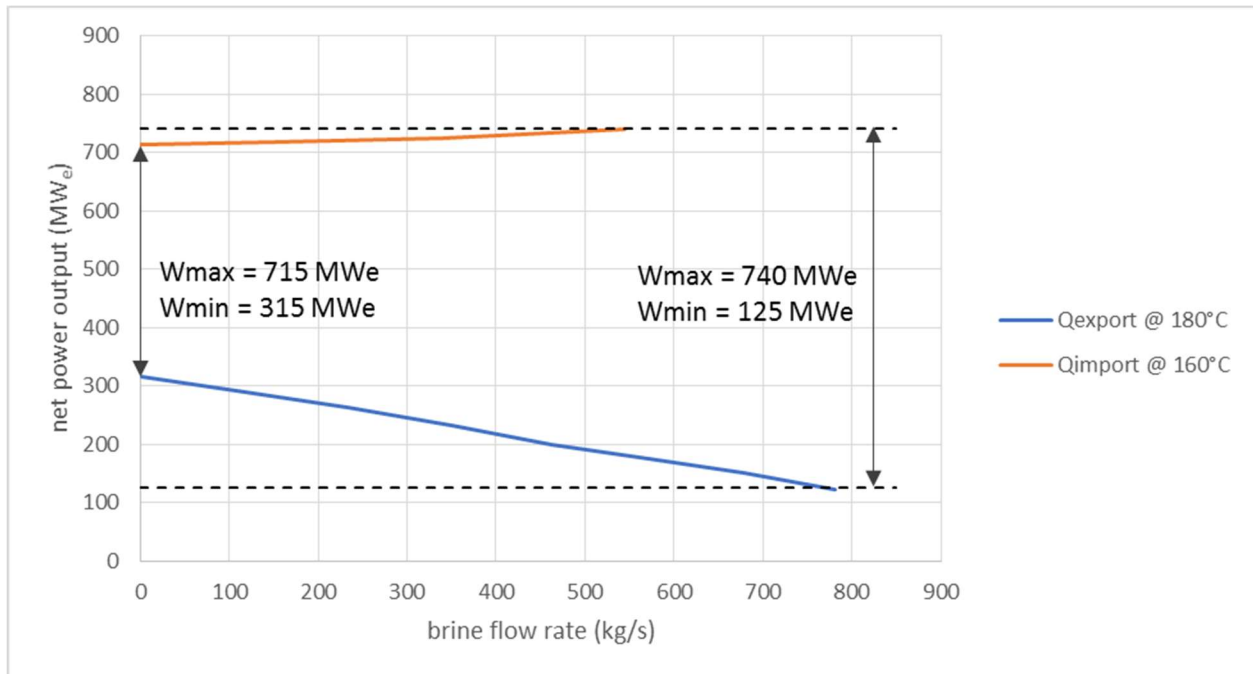


Figure 13. Coupling a coal-fired power plant with a GeoTES system would allow increased electrical power generation during periods of high demand and decreased electrical power generation during periods of low demand.

The minimum and maximum electrical power generation of the coal-fired power plant when coupled with a GeoTES system operating at a temperature of 160°C was evaluated. For this evaluation, it was assumed that the temperature of the heated brine exported from the coal-fired power plant was 180°C to account for thermal losses in the piping network as well as the GeoTES reservoir. The temperature of the brine recovered from the GeoTES reservoir was assumed equal to the GeoTES operating temperature of 160°C. As illustrated in Figure 13, the coal-fired power plant operating without heat transfer to/from the GeoTES system has a maximum net power generation of 715 MW$_e$ and a minimum power generation of 315 MW$_e$ (assuming 50% MCL for boiler operation), resulting in 400 MW$_e$ of ramping capacity. However, the coal-fired power plant coupled with a GeoTES system has a maximum power generation of 740 MW$_e$ and a minimum power generation of 125 MW$_e$, resulting in 615 MW$_e$ of ramping capacity.

Coupling the 715 MW$_e$ nameplate capacity coal-fired power plant with a GeoTES system could therefore potentially increase ramping capacity by 215 MW$_e$, which is equivalent to a 54% increase. It is expected that similar increases in ramping capacity would be achievable for similarly configured coal-fired power plants with different nameplate capacities.

Figure 13 illustrates that the flow rate of heated brine to the GeoTES system for energy storage is greater than the flow rate of heated brine from the GeoTES system for energy recovery. The implication is that, in the coal-fired power plant application, heat could be stored at a rate greater than it could be utilized upon recovery. This characteristic could be leveraged in one or more of the following ways: (a) enable operation for a greater percentage of time in the high output mode than the low output mode, (b) allow the system to be more robust with regard to potential thermal losses during energy storage, and/or (c) the stored energy could be recovered for multiple end uses, e.g., heat input to a direct use geothermal application (such as district heating or agricultural product drying) in addition to heat input to a coal-fired power plant. A more detailed evaluation of potential system operating modes and alignment with market demands is planned as a Phase II analysis task.

## 6.  GRID STABILITY-IMPLICATIONS MODELING (UI ROBERSON):

Classically, the electric generation, transmission, and distribution system hierarchy has followed a rigid model – electricity generated remotely by synchronous machines (i.e., generators) is transmitted through medium and long distances at high voltage to be distributed to consumer loads at low voltage for consumption. Distributed generation, including rooftop solar and wind turbines, prove disruptive to this hierarchy as they generate electricity (typically) at the distribution level. Independent system operators, regional transmission operators, and utility partners with a stake in the large interconnected systems which make up our grid are paying close attention to the potential impact these changes have on overall power system stability.

Further complication from the power system stability perspective is apparent in the rapid retirement of large fossil fuel-powered generators. By replacing deterministic generating capabilities with largely stochastic power electronics-based systems at the distribution level, synchronism between the remaining generators (a critical concept to stability) is of concern. Synchronism is largely a function of generator loading, closely associated with the complex mixture of generation/load mismatch, nominal generator operating conditions, and the availability of standby sources of generation.

Generator inertia associated with the generator rotor mass and velocity play a key role in the fundamental instability phenomenon associated with these dynamics. In general, a generator with more inertia is typically more insensitive to changes in the electromagnetic stator field and prime mover disturbances than a similar generator with less inertia. Complicating the concept is the idea that *groups of generators* may remain synchronized with one another while simultaneously opposing synchronization with others in the same system. These dynamics are of particular concern in the Western Interconnect (WI) where large coal generators, for example, are found in the far north and eastern regions (Wyoming, Montana, Alberta) supporting significant load in the Southwest (California and Las Vegas, NV, for example).

The decommissioning of coal-fired units in these remote areas may adversely impact these dynamics, increasing the likelihood of rotor stability issues if left unaccounted for. Because power electronic devices have inherently no inertia, replacing the synchronous machine with an equivalent solar array, for example, tends not to be a zero-sum exchange. Initial results provided herein indicate that inertia-based generators are particular interest to those concerned with the stability of a grid in the midst of a paradigm shift with respect to generation/transmission/distribution configurations.

# 6.1   Linear Stability Dynamics

The study of rotor stability is concerned with the continued synchronization of all generator rotors in an interconnected electric grid. The fundamental laws that govern generator synchronism are associated with a torque imbalance between the electrical, magnetic, and mechanical components of the generators. Since electricity is generated and consumed simultaneously at all instances in time, generation and load equilibrium is key to ensure minimal torque imbalance. To illustrate the concept, consider a single generator connected to an infinitely rigid system by impedance $Z = R + jX$, as in Figure 19.
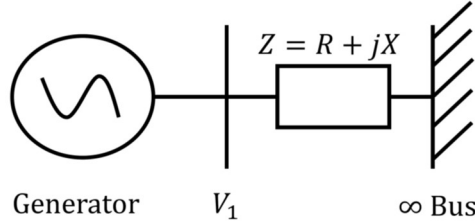


Figure 19: Single machine infinite bus model.

With respect to the Newtonian physics of this classical generator model for purposes of illustration, rotor acceleration is given by

$$J \frac{d\omega_m}{dt} = T_a = T_m - T_e,$$

where $J$ is the combined moment of inertia of the generator and turbine in $kg * m^2$; $\omega_m$ is the angular velocity of the rotor in mechanical $rad/sec$; and $T_a, T_m, and\ T_e$ are the accelerating, mechanical and electrical torque in $Nm$, respectively. Thus, the rotational velocity of the generator remains at equilibrium (i.e., its derivative is zero) if no accelerating torque is applied. Linearizing and rewriting in terms of "rotor angle" and a normalized inertia constant,

$$\frac{2H}{\omega_0} \frac{d^2\delta}{dt^2} = T_m - T_e - K_d \Delta\omega_r,$$

where $H$ is the generator's normalized "inertia constant", $\delta$ the internal rotor angle (first time derivative of rotor velocity), $K_d$ a proportional term related to damping, and $\Delta\omega_r$ are small perturbations in the rotational velocity. A state-space representation of this governing equation is often useful for illustrating the dynamics associated with the generator's oscillatory behavior with respect to the infinite bus. The state equations become

$$\frac{d\omega_r}{dt} = \frac{1}{2H} (T_m - T_e - K_d \Delta\omega_r)$$

and

$$\frac{d\delta}{dt} = \omega_0 \Delta\omega_r$$

where all variables are normalized except time and $\omega_0$, the rated generator frequency. A block diagram of this decomposition follows (Figure 20):
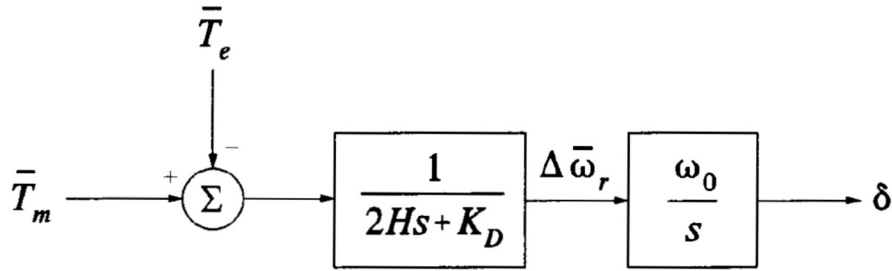
Figure 14. Block diagram of classical generator model.

While this model is simplified, it provides a basis for the oscillatory phenomenon of interest in large multimachine systems. To illustrate, consider the previous equations arranged in the state space model analogous to a mass spring damper (MSD) system $M\frac{d^2 y}{dt^2} + D\frac{dy}{dt} + Ky = u$, where $u$ is input force, $y$ the mass position (output), and $M, D, K$ the mass, damp rate, and spring stiffness constants (respectively). The states, then, are given by $x_1(t) = y(t), \dot{x}_{1(t)} = x_2(t) = \frac{dy(t)}{dt}$, and $\dot{x}_2(t) = \ddot{x}_1(t) = \frac{d^2 y(t)}{dt^2}$. The state differential equation, then, is given by

$$\begin{bmatrix} \dot{x}_1 \\ \dot{x}_2 \end{bmatrix} = \begin{bmatrix} a_{11} & a_{12} \\ a_{21} & a_{22} \end{bmatrix} \begin{bmatrix} x_1 \\ x_2 \end{bmatrix} + \begin{bmatrix} b_1 \\ b_2 \end{bmatrix} u$$

$$= \begin{bmatrix} 0 & 1 \\ -K/M & -D/M \end{bmatrix} \begin{bmatrix} x_1 \\ x_2 \end{bmatrix} + \begin{bmatrix} 0 \\ 1/M \end{bmatrix} u$$

where input is force applied to mass $u = f$, and

$$y = [1\ 0][x_1 x_2]^T.$$

Generally, therefore, the *state space realization* of an *n*-state LTI sys. w/ *m*-inputs and *l*-outputs is the *(A,B,C,D)* matrix quadruple:

A = state matrix

B = input shaping matrix

C = output shaping matrix

D = input feed-through matrix

where

$$\dot{x} = Ax(t) + Bu(t)$$

$$y = Cx(t) + Du(t).$$

The value of this representation is not obvious, but upon closer inspection, the eigenproperties of the dynamic system reveal the stability characteristics of the (linearized) power system. Solving the equation $(A-\lambda I)\phi=0$ for all $\lambda = \sigma + j\omega$ yields the *characteristic roots* (i.e., the roots of the characteristic equation), revealing the underlying stability of the system.

This simple dynamic representation of the MSD system provides insight into the power system rotor stability phenomena. Application of this model format to the first order differential equations representing rotor angle and rotational velocity yields

$$\frac{d}{dt}\begin{bmatrix}\Delta\omega_r\\\Delta\delta\end{bmatrix} = \begin{bmatrix}-\dfrac{K_D}{2H} & -\dfrac{K_s}{2H}\\\omega_0 & 0\end{bmatrix}\begin{bmatrix}\Delta\omega_r\\\Delta\delta\end{bmatrix} + \begin{bmatrix}\dfrac{1}{2H}\\0\end{bmatrix}\Delta T_m,$$

Which is of identical form to $\dot{x} = Ax + Bu$. The second order solution which governs the response of a complex pair of eigenvalues of the state matrix yields two values of interest: the undamped natural frequency and the damping ratio,

$$\omega_n = \sqrt{\left(\frac{K_s\omega_0}{2H}\right)}\ \text{[rad/s]}$$

$$\zeta = \frac{0.5K_D}{2H\omega_n} = \frac{0.5K_D}{\sqrt{K_s 2H\omega_0}} = -\frac{\sigma}{\sqrt{\sigma^2 + \omega^2}}$$

Each of these parameters are functions of the eigenvalue location in the complex plane; thus, eigenanalysis of the state matrix reveals stability characteristics readily (i.e., oscillatory instability occurs for $\zeta < 0$).

Due to the liberal assumptions applied thus far (for illustrative purposes), the above logic holds for the classical SMIB generator model. However, incorporation of the rotor (field) dynamics, exciter and automatic voltage regulator dynamics, and power system stabilizer results in a far more complex state matrix, even in the SMIB context. Translated to a multimachine system while incorporating load and transmission dynamics further complicates the model. Therefore, it is sufficient for the scope of this document to suggest that eigenanalysis (also referred to as modal analysis) will provide insight into the stability of the system by inspection of the eigenvalues, associated left and right eigenvectors, and participation factors. Interested readers are encouraged to review Kundur, 1994, for additional information on the model.

For completeness, the modal decomposition (i.e., diagonalization) of the state matrix is of the form

$$\Psi A\Phi = \Phi^{-1}A\Phi = \Lambda,$$

where $\Phi$ is the *right modal matrix* consisting of the right eigenvectors arranged in matrix form while the left eigenvectors are arranged in matrix form to form the *left modal matrix* $\Psi$. $\Lambda$ is the diagonal matrix of eigenvectors. From this decomposition, several other valuable definitions are assumed, the most valuable of which is the *participation matrix*

$$P = \begin{bmatrix} p_1 & p_2 & \cdots & p_n \end{bmatrix}$$

where

$$p_i = \begin{bmatrix} p_{1i}\\ p_{2i}\\ \cdots \\ p_{ni}\end{bmatrix} = \begin{bmatrix} \phi_{1i}\psi_{i1}\\ \phi_{2i}\psi_{i2}\\ \cdots \\ \phi_{ni}\psi_{in}\end{bmatrix}.$$

The participation matrix is of particular interest as it combines left and right eigenvectors as a net measure of association between state variables and dynamic modes (oscillatory behavior) of the system while normalizing.

## 6.2   Mode Types

Oscillatory modes of the large multi-machine system are not confined to a single machine rotor speed oscillating with respect to an infinite bus; instead, multi-area dynamics are of utmost concern, as are oscillations specific to the rotor shaft itself (i.e., torsional modes). To summarize, a classification of four oscillation types is considered:

1. Local Modes (0.8-4.0 Hz)

- 'Swinging' of units at a generator with respect to the rest of system (SMIB)
- Instability of this type of mode typically results in removal of a single unit from system

2. Control Oscillations
   - Associated with individual generators and poorly tuned controllers
   - Can typically be fixed locally, are difficult to analyze in toto

3. Inter-area oscillations (0.1-1.0 Hz)
   - Groups of generators oscillate against other groups of generators
   - Pernicious in large, geographically disparate systems
   - May lead to large, cascading blackouts and/or system islanding (e.g., August 1996)

4. Torsional Modes (4.0-20 Hz)
   - Turbine-generator shaft torque imbalance due to high, intermediate, and low-pressure turbine stages.
   - Often lightly damped, high frequency, and can ruin turbine shafts on thermal units (hydroelectric generators are sufficiently stiff with equally distributed loading to be of little concern)
   - Exacerbated by poorly tuned local controllers

A simple depiction of the torsional shaft mode phenomenon is shown below (Figure 21), indicating the high, intermediate, and low-pressure shaft inputs. The shaft is not infinitely rigid; torque imbalance between the different inputs results in the oscillatory behavior described above and is expected to be exacerbated with rapid steam diversion for GeoTES purposes (to be investigated in future work).
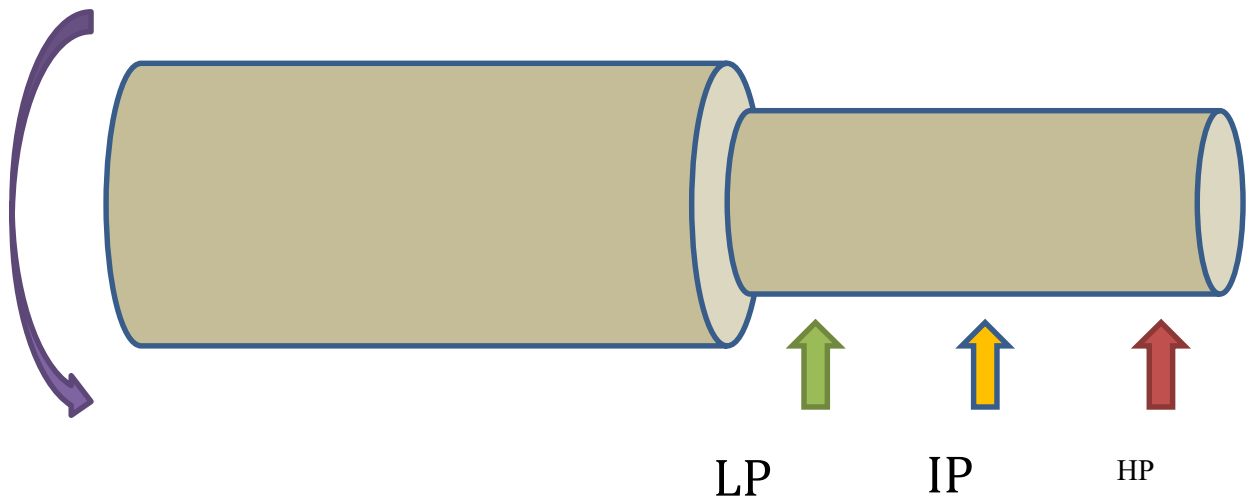


Figure 21. Schematic depiction of the torsional shaft mode phenomenon, indicating high, intermediate, and low-pressure shaft inputs.

In the context of power system stability, inter-area oscillations frequently present the widest-ranging negative impact, resulting in reduction in transmission line flows and the potential for system-wide destabilization. In this study, all mode types are evaluated.

Practical analysis of the linear rotor stability of the system follows the following architecture:

1. Develop linear state space model:

a. Model each individual generator in the system, relative to its own frame of reference, including accounting for each of the following:
    i. Newtonian physics (acceleration/swing equation, as shown above),
    ii. Rotor circuit equations,
    iii. Field effects,
    iv. Excitation system,
    v. Prime mover and/or governor dynamics.
b. Model transmission network and static loads
c. Model dynamic loads, including:
    i. Induction motors
    ii. Constant current/power/impedance loads
    iii. Dynamic loads
d. Develop common frame of reference
e. Transform all parameters to common frame of reference
2. Diagonalize state space model
3. Analyze modal properties
    a. Eigenvalue locations in complex plane
    b. Frequency/damping of each eigenvalue
    c. For eigenvalues of concern (i.e., low damping ratio):
        i. Determine their "type" (one of four classifications described)
        ii. Analyze participation/sensitivity/etc. to determine trends associated with this oscillatory activity
        iii. Identify generator(s) which contribute positively or negatively to the behavior
4. If necessary, transient stability analysis (outside initial scope of work shown here)
    a. Time-domain solution of the nonlinear differential governing equations
    b. High computational complexity

Several open source and commercial software packages are particularly helpful for the analysis above. Power System Toolbox is an open source platform used for the initial linear provided here using a reduced-order model of the WI. Power World Dynamic Studio with full-scale Western Electric ordinating Council (WECC) planning cases is recommended for future analysis using a more detailed model framework, including full-scale nonlinear (transient) analysis. A one-line diagram of the reduced-order model used here is depicted in Figure 22.
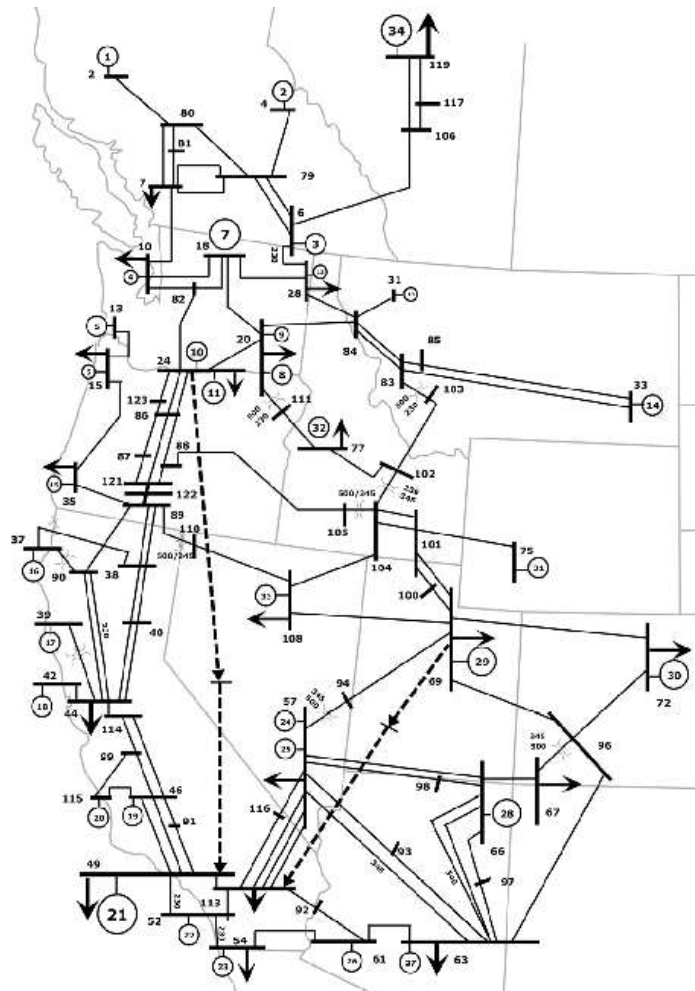
Figure 15. One-line diagram for Power System Toolbox simulation of the WI.

## 6.3    Preliminary Findings

Following the detailed analysis plan provided above, an investigation into the impact of removal and/or modification of the inertia associated with the Jim Bridger plant in western Wyoming follows. The dynamic mode of most concern is the "North-South Mode" associated with groups of generators in Canada and the Pacific Northwest exchanging accelerating torque $T_a$ with those in Arizona, Colorado, and Wyoming. To visualize, consider the two MSD systems below (Figure 23):
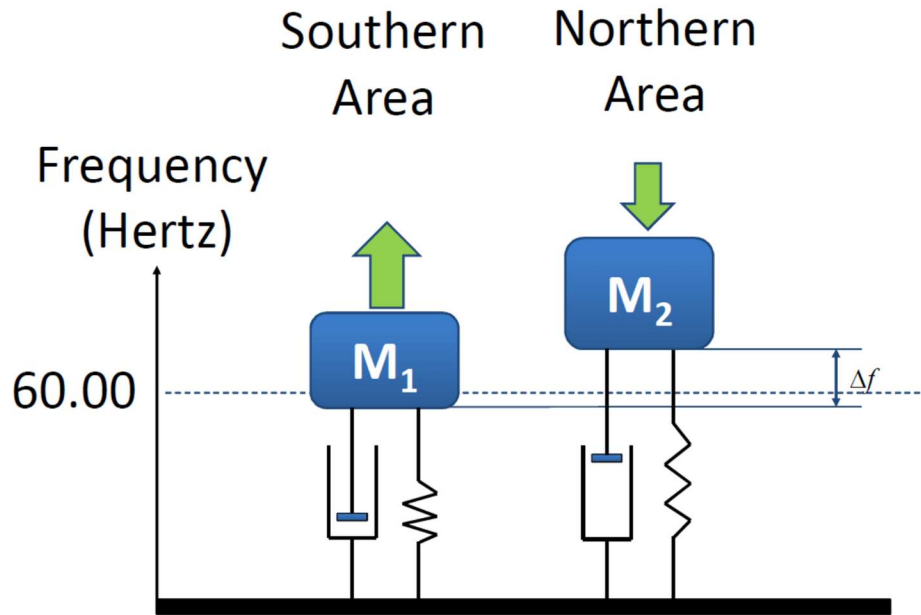
Figure 23. MSD system representing the northern and southern portions of the WI.

Generator groups are color-coded in Figure 24 to show the generator groupings (in general terms):
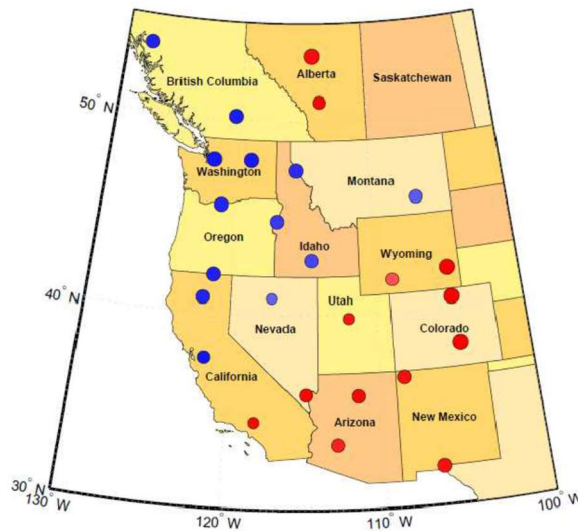


Figure 24. Generator groups for the WI – colors depict two general geographic groupings of power plants (red and blue).

Changes in inertia in Southern Wyoming (i.e., Jim Bridger) resultant from generator decommissioning, steam diversion for GeoTES purposes, and operational reconfiguration present a slight increase in modal frequency and a large decrease in modal damping. This shift presents a significant concern to power system stability, suggesting that a decrease in inertia in the southern area of the system causes the "stiffness" of the springs in the MSD system above to increase. In other words, the southern

area is more sensitive to oscillations induced in the north and vice versa, causing an exaggerated system-wide oscillation at 0.35 Hz.

# 7. SUMMARY

This Phase I project evaluated the viability of the GeoTES concept for storing subsurface sedimentary basins, with geographically distributed analogues, to store excess heat collected from large thermal power stations during non-peak or high renewable production. The project team evaluated the topside and subsurface technical aspects required to recover and generate flexible geothermal energy from the geothermally stored heat. The grid-scale energy storage that could be provided by GeoTES technology would enable the grid to continue operating in the face of legislatively mandated increases in the percentage of renewable energy on the U.S. grids, while positively impacting overall grid stability and reliability.

Heat storage and recovery performance of a GeoTES system was analyzed for a representative sedimentary formation confined between cap and base rock layers. The GeoTES operating temperature was initially specified as at temperatures >160°C. This operating temperature range would allow a GeoTES system to accept heat from important conventional Rankine cycle heat and low-carbon (i.e., solar thermal, nuclear, etc.) sources. Thereby providing a heat recovery temperature high enough to enable increased power cycle efficiency.

Several well field configurations were investigated, including single and five-spot well patterns. In order to maintain the brine liquid phase, a target reservoir depth of up to 1,200 meters (4,000 feet) was specified for subsurface simulations. Phase I results indicate that a preferred GeoTES well configuration involves five-spot well patterns with dedicated hot and cold wells to efficiently cycle the geothermal brine from injection to recover wells. This configuration allowed immediate recovery of the hot fluid stored in a GeoTES reservoir while providing a practical approach for managing the system's fluid inventory, increasing thermal recovery, and reducing parasitic load. The production pumping requirements were reduced through pressure support provided by the wells operating in "push" mode to the wells operating in "pull" mode. As a result of this work, considerable effort needs to be expended to evaluate the thermal-hydraulic, mechanical-chemical implications, and potential mitigation approaches to storing energy as heated bring in geologic reservoirs.

Geochemical effects of increasing the host reservoir from its ambient temperature of ~80°C to temperatures greater than 160°C were also investigated. For the geochemical evaluation, we selected the Weber/Tensleep Formation in Wyoming's Rock Springs Uplift, a representative siliciclastic analogue for our GeoTES application in North America and the project team has considerable characterization data. In this application, the coupled fluid and heat flow in the storage reservoir were numerically simulated, with results suggesting that with the highly saline water (>35,000 mg/L) composition considered. Our Phase I results indicate that with increasing GeoTES temperature scaling may be expected both in the surface equipment installed to heat the extracted water and around injection wells. Further studies are needed to assess (1) the scaling potential of other, possibly more dilute formation waters or waters from different geological and hydrological settings, (2) the use of anti-scalants and their potential effects on the economics of the GeoTES operation, and (3) extraction/injection scenarios that minimize the scaling potential.

The major take-away points from out Phase I project are:

- GeoTES systems could be installed at many locations distributed throughout the country. The distributed nature of these installations would increase grid stability through minimizing risks associated with transmission and grid dynamics, as well as to also provide numerous installations to minimize system impact in the case of an outage at one installation. Further, each installation would use turbines for power generation; the inherent rotational inertia associated with turbines would provide grid stability benefits not available through use of electrochemical batteries.

- The temperature of GeoTES working fluid (brine) impacts the volume of fluid that must be transported to meet heat transfer requirements; higher temperature enables greater quantities of heat to be transferred between the power plant and GeoTES system, but has implications for GeoTES system operation

- Heat extraction from steam Rankine cycles can significantly reduce electrical power output during periods of low electrical demand; this heat could be diverted to a large capacity GeoTES system for storage and subsequent utilization for increasing electrical power output during periods of high electrical demand. Exporting 180°C heat from a coal-fired power plant (operating at 50% MCL) to a GeoTES system during periods of low electrical demand could reduce electrical power output by approximately 60% when compared to a plant with no TES capacity.

  - A steam Rankine cycle power plant steam bypass system can provide high rate of heat export; the heat input rate via the feed water heating system is smaller in magnitude but still significant with regard to providing additional power plant ramping capacity. The net effect is that large quantities of heat could be stored relatively quickly and then recovered over longer time periods (amenable to seasonal energy storage).

- Stored heat could be input to steam Rankine cycle during full load operation to increase net power output. The temperature of the brine recovered from the GeoTES dictates the potential increase in power generation; GeoTES brine recovered at a temperature greater than 160°C could increase the maximum net power generation by approximately 3.5%.

- The flow rates of brine required to store and recover heat from a GeoTES system coupled with a 715 MWe coal-fired power plant are comparable to those for a ~50 MW geothermal binary power plant

- In the current market, the MCL restriction may force the large power plants to go offline during periods when there is an oversupply of renewable power available. However, coupling the steam Rankine cycle to a GeoTES system would allow the power plants to operate with a lower electrical power output than is currently possible, since a portion of the heat would be diverted to the GeoTES system instead of to the steam turbines. This low-output power plant operating strategy would maintain the electro-mechanical coupling of the steam turbines (high rotational inertia) to the electrical grid to enhance grid stability and reliability.

- Use of GeoTES for heat storage coupled with an appropriate power cycle provides a unique and fully dispatchable seasonal energy storage capability that can provide the foundation to support energy markets with large quantities of variable renewable energy sources. This unique capability provides a potential pathway to helping electricity suppliers access grid scale energy storage while maintaining grid reliability

# 8.   FUTURE WORK

The geochemical results of the Phase I projects suggest scaling the highly saline water composition found in GeoTES targeted reservoirs may be an issue in the subsurface geology and the surface equipment installed to heat the extracted brine. Therefore, the proposed Phase II project will focus further studies to assess (1) scaling potential of other, possibly more dilute formation waters in the area, which may then require evaluating different geological and hydrological settings, (2) use of anti-scalants and their potential effects on the economics of the TES operation, and (3) extraction/injection scenarios that minimize the scaling potential

The initial preliminary reservoir flow and thermal storage simulations, with highly simplified reservoir geological configurations, were performed during Phase I for the proof of concept of GeoTES. The initial simulation results clearly indicate that a large number of parameters, including reservoir flow and thermal properties, injection rate and injection temperature, initial reservoir temperature, aqueous

geochemistry and potential mineral precipitations, well configurations, influence the recovery efficiency of thermal energy stored in GeoTES reservoirs. These initial reservoir thermal storage simulations also demonstrate that certain combinations of reservoir flow properties, well configurations and injection/production strategies, could lead to very promising high thermal recovery efficiency, while minimizing formation effects and show the GeoTES concept is a very promising for large-scale underground TES and recovery. However, these initial subsurface modeling studies also demonstrate the need for more comprehensive reservoir simulation studies to (1) optimize the GeoTES reservoir operating strategy for maximizing the recovery of stored thermal energy in various representative reservoirs with realistic flow properties; (2) achieve better understanding of the effects of potential mineral precipitations on reservoir permeability and wellbore injectivity for various representative reservoirs; and (3) reliably predict reservoir geomechanical response to large-scale underground thermal storage and temperature cycling, including the potential induced seismicity risk.

During Phase I, a Rankine steam offtake model was developed to evaluate the technical and economic potential of GeoTES when integrated with a geothermal energy storage scenario. The model was applied to assess various types of power cycles and the dual-flash steam cycle was identified as the most efficient cycle when coupled with the GeoTES system at a design temperature of 250°C. The initial study also showed that the system levelized cost of energy decreased with increasing storage capacity. Recommendations for Phase II work would be to investigate more detailed system designs by incorporating electrical power dispatch data and assess the economic viability of GeoTES-based flexible power generation systems

An initial power system stability analysis was performed during Phase I to better understand and begin to quantify the first principles physics-based relationships between thermal generator kinetic energy (i.e., inertia) and machine synchronism in the GeoTES context. Under current operational conditions, generator synchronism may become strained with a reduction in kinetic energy, particularly in areas of a large electrical grid which are connected through long non-redundant transmission corridors (e.g., large thermal power plants, such as Palo Verde, AZ; Colstrip, MT; or Jim Bridger, WY). The initial modeling indicates that with the addition of GeoTES, these large generators may be safely operated in a low output mode and remain capable of rapid increases in generation without harm to plant equipment. However, additional analysis is necessary to better understand the impact of reduced inertia on several other stability metrics as they relate to diverted thermal energy to a GeoTES reservoir. These stability metrics include the system's ability to maintain frequency stability in the face of large transient events (e.g., transmission line faults), as well as voltage and reactive power support, for example. Thermo-electric power plant heat diversion strategies considered in the Phase I study may have other previously unstudied impact on turbine dynamics such as torsional vibrations and premature wearing of rotor components and will be studied comprehensively.

# 9. REFERENCES

Hunter, K., Bielicki, J.M., Middleton, R., Stauffer, P., Pawar, R., Harp, D. and Martinez, D., 2017. Integrated CO2 Storage and Brine Extraction. *Energy Procedia*, *114*, pp.6331-6336.

Jiao, Z., Pawar, R., Duguid, A., Bourcier, W., Haussmann, C., Coddington, K., Harp, D., Ganshin, Y., Quillinan, S., McLaughlin, F. and Ramsey, R., 2017. A Field Demonstration of an Active Reservoir Pressure Management through Fluid Injection and Displaced Fluid Extraction at the Rock Springs Uplift a Priority Geologic CO2 Storage Site for Wyoming. *Energy Procedia*, *114*, pp.2799-2811.

Frost, C.D., McLaughlin, J.F., Frost, B.R., Fanning, C.M., Swapp, S.M., Kruckenberg, S.C. and Gonzalez, J., 2017. Hadean origins of Paleoarchean continental crust in the central Wyoming Province. *Bulletin*, *129*(3-4), pp.259-280.

Litynski, J.T., Klara, S.M., McIlvried, H.G., Srivastava, R.D. The United States Department of Energy's Regional Carbon Sequestration Partnerships program: A collaborative approach to carbon management, *Environment International*, 32 (2006) 128-144 http://dx.doi.org/10.1016/j.envint.2005.05.047.

McLaughlin, J.F. and Garcia-Gonzalez, M., 2013. Detailed Geologic Characterization of Core and Well Data from the Weber and Madison Formations and Associated Seals at a Potential $CO_2$ Sequestration Site in Southwest Wyoming: Defining the Lithologic, Geochemical, Diagenetic, and Burial Histories Relative to Successful $CO_2$ Storage. In *Geological CO2 storage characterization* (pp. 55-96). Springer, New York, NY.

Stauffer, P.H., R.C. Surdam, Z. Jiao, T.A. Miller, and R.D. Bentley, 2009. Combining geologic data and numerical modeling to improve estimates of the $CO_2$ sequestration potential of the Rock Springs Uplift, Wyoming. Energy Procedia 1, GHGT-9, 2717-2724.

C. Surdam, Ronald & Jiao, Zunsheng & Stauffer, Philip & Miller, T. (2011). The key to commercial-scale geological CO 2 sequestration: Displaced fluid management. Energy Procedia. 4. 4246-4251. 10.1016/j.egypro.2011.02.373.

SimTech GmbH, "IPSEpro Process Simulation Environment," Version 7.0 U, Release 12, Build 1744 ed, 2017.

M. A. Gonzalez-Salazar, T. Kirsten, and L. Prchlik, "Review of the operational flexibility and emissions of gas- and coal-fired power plants in a future with growing renewables," *Renewable and Sustainable Energy Reviews,* vol. 82, pp. 1497-1513, 2018.